Targeted Genome Editing of Bacteria Within Microbial Communities

Benjamin E. Rubin[1,2,13], Spencer Diamond[1,3,13], Brady F. Cress[1,2,13], Alexander Crits-Christoph[4], Christine He[1,2,3], Michael Xu[1,2], Zeyi Zhou[1,2], Dylan C. Smock[1,2], Kimberly Tang[1,2], Trenton K. Owens[5], Netravathi Krishnappa[1], Rohan Sachdeva[1,3], Adam M. Deutschbauer[4,5], Jillian F. Banfield[1,3,6,7]* & Jennifer A. Doudna[1,2,8-12]*

[1]Innovative Genomics Institute, University of California, Berkeley, CA, USA. [2]Department of Molecular and Cell Biology, University of California, Berkeley, CA, USA. [3]Department of Earth and Planetary Science, University of California, Berkeley, CA, USA. [4]Department of Plant and Microbial Biology, University of California, Berkeley, CA, USA. [5]Environmental Genomics and Systems Biology Division, Lawrence Berkeley National Laboratory, Berkeley, California, USA. [6]Environmental Science, Policy and Management, University of California, Berkeley, CA, USA. [7]School of Earth Sciences, University of Melbourne, Melbourne, Victoria, Australia. [8]California Institute for Quantitative Biosciences, University of California, Berkeley, CA, USA. [9]Department of Chemistry, University of California, Berkeley, CA, USA. [10]Howard Hughes Medical Institute, University of California, Berkeley, CA, USA. [11]Molecular Biophysics & Integrated Bioimaging Division, Lawrence Berkeley National Laboratory, Berkeley, CA, USA [12]Gladstone Institutes, University of California, San Francisco, CA, USA. [13]These authors contributed equally to this work: Benjamin E. Rubin, Spencer Diamond, Brady F. Cress.

*e-mail: doudna@berkeley.edu; jbanfield@berkeley.edu

Knowledge of microbial gene functions comes from manipulating the DNA of individual species in isolation from their natural communities. While this approach to microbial genetics has been foundational, its requirement for culturable microorganisms has left the majority of microbes and their interactions genetically unexplored. Here we describe a generalizable methodology for editing the genomes of specific organisms within a complex microbial community. First, we identified genetically tractable bacteria within a community using a new approach, Environmental Transformation Sequencing (ET-Seq), in which non-targeted transposon integrations were mapped and quantified following community delivery. ET-Seq was repeated with multiple delivery strategies for both a nine-member synthetic bacterial community and a ~200-member microbial bioremediation community. We achieved insertions in 10 species not previously isolated and identified natural competence for foreign DNA integration that depends on the presence of the community. Second, we developed and used DNA-editing All-in-one RNA-guided CRISPR-Cas Transposase (DART) systems for targeted DNA insertion into organisms identified as tractable by ET-Seq, enabling organism- and locus-specific genetic manipulation within the community context. These results demonstrate a strategy for targeted genome editing of specific organisms within microbial communities, establishing a new paradigm for microbial manipulation relevant to research and applications in human, environmental, and industrial microbiomes.

Genetic mutation and observation of phenotypic outcomes are the primary means of deciphering gene function in microorganisms. This classical genetic approach requires manipulation of isolated species, limiting knowledge in three fundamental ways. First, the vast majority of microorganisms have not been isolated in the laboratory and are thus largely untouched by molecular genetics[1]. Second, emergent properties of microbial communities that may arise due to interactions between their constituents, remain mostly unexplored[2]. Third, microorganisms

48 grown and studied in isolation quickly adapt to their new lab environment, obscuring their true
49 "wild type" physiology[3]. Since most microorganisms relevant to the environment, industry and
50 health live in communities, approaches for precision genome modification (editing) in community
51 contexts will be transformative.

52 Advances toward genome editing within microbial communities have included assessing
53 gene transfer to microbiomes using selectable markers[4–9], microbiome manipulation leveraging
54 pre-modified isolates[10], and use of temperate phage for species-specific integration of genetic
55 payloads[11]. However, a generalizable strategy for programmable organism- and locus-specific
56 editing within a community of wild-type microbes has not yet been reported[12].

57 Here we show that specific organisms within microbial communities can be targeted for
58 site-specific genome editing, enabling manipulation of species without requiring prior isolation or
59 engineering. Using a new method developed for this study, Environmental Transformation
60 Sequencing (ET-Seq), we identified genetically accessible species within a nine-member
61 synthetic community and among previously non-isolated species in a 197-member bioremediation
62 community. These results enabled targeted genome editing of microbes in the nine-member
63 community using DNA-editing All-in-one RNA-guided CRISPR-Cas Transposase (DART)
64 systems developed here. The resulting species-specific editing provides the first broadly
65 applicable strategy for organism- and locus-specific genetic manipulation within a microbial
66 community, hinting at new emergent properties of member organisms and methods for controlling
67 microorganisms within their native environments.

68

69 **ET-Seq detects genetically accessible microbial community members**

70 Editing organisms within a complex microbiome requires knowing which constituents are
71 accessible to nucleic acid delivery and editing. We developed ET-Seq to assess the ability of
72 individual species within a microbial community to acquire and integrate exogenous DNA (Fig.
73 1a). In ET-Seq, a microbial community is exposed to a randomly integrating mobile genetic

element (here, a *mariner* transposon), and in the absence of any selection, total community DNA is then extracted and sequenced using two protocols. In the first, we enrich and sequence the junctions between the inserted and host DNA to determine insertion location and quantity in each host. This step requires comparison of the junctions to previously sequenced community reference genomes. In the second, we conduct low-depth metagenomic sequencing to quantify the abundance of each community member in a sample (Extended Data Fig. 1a). Together these sequencing procedures provide relative insertion efficiencies for microbiome members. To normalize these data according to a known internal standard, we add to every sample a uniform amount of genomic DNA from an organism that has previously been transformed with, and selected for, a *mariner* transposon. In the internal standard, we expect every genome to contain an insertion. The final output of ET-Seq is a fractional number representing the proportion of a target organism's population that harbored transposon insertions at the time DNA was extracted, or insertion efficiency (Extended Data Fig. 1b). To facilitate the analysis of these disparate data, we developed a complete bioinformatic pipeline for quantifying insertions and normalizing results according to both the internal control and metagenomic abundance (https://github.com/SDmetagenomics/ETsuite and Methods). Together the experimental and bioinformatic approaches of ET-Seq reveal species-specific genetic accessibility by measuring the percentage of each member of a given microbiome that acquires a transposon insertion.

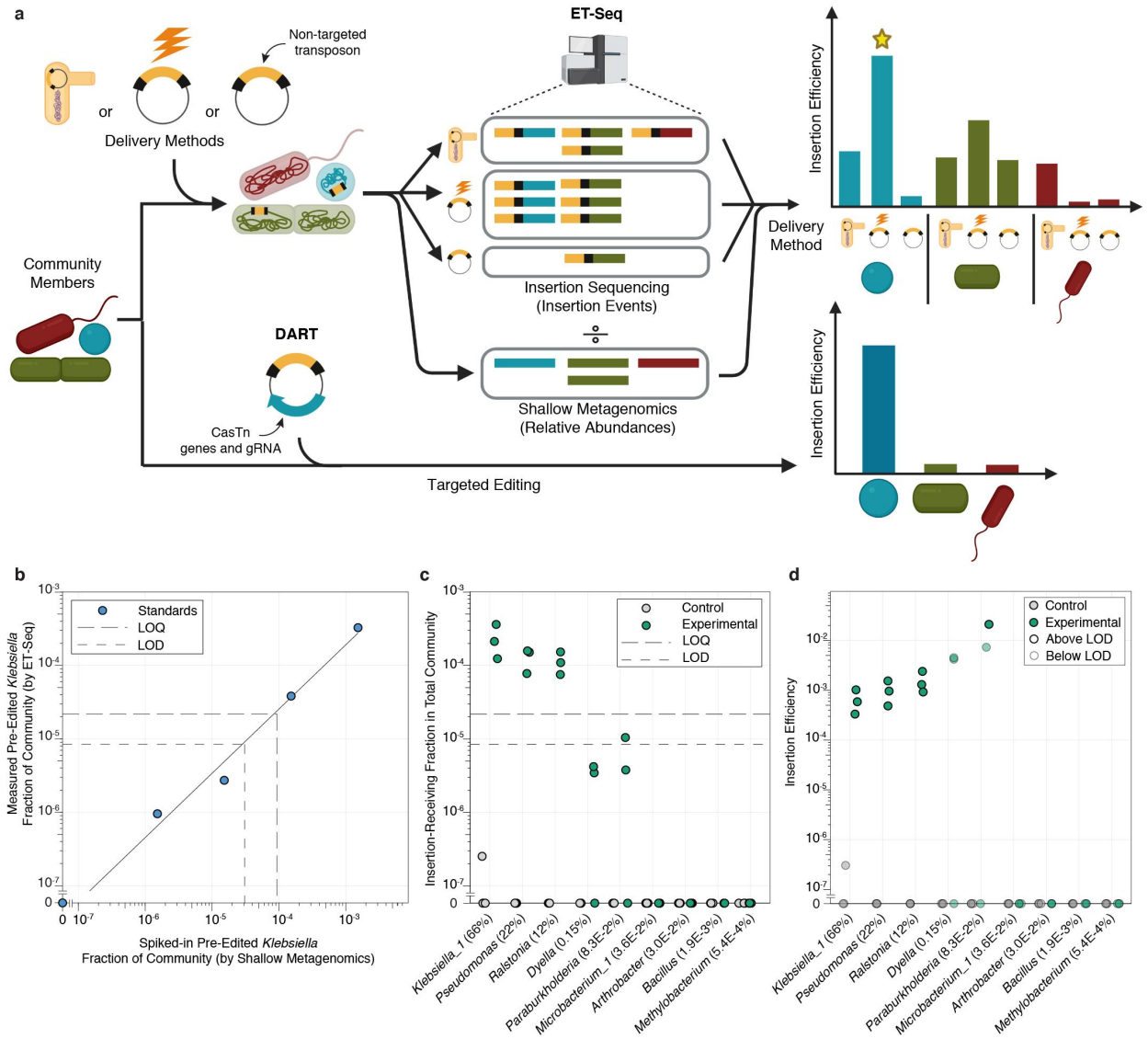

Fig. 1 | ET-Seq for quantitative measurement of insertion efficiency in a microbial community. a, ET-Seq provides data on insertion efficiency of multiple delivery approaches, including conjugation, electroporation, and natural DNA transformation, on microbial community members. In this illustrative example, the blue strain is most amenable to electroporation (star). This data allows for the determination of feasible targets and delivery methods for DART targeted editing. **b,** ET-Seq determined efficiencies for known quantities of spiked-in pre-edited *K. michiganensis* (*Klebsiella_1*). Data shown is the mean of three technical replicates. LOD is the lowest insertion fraction at which accurate detection of insertions is expected and LOQ is the lower limit at which this fraction is expected to be quantifiable. Solid line is the fit of the linear regression to the data not including zero (n = 4 independent samples) that is used to calculate

103 LOD and LOQ (slope = 0.2137; intercept = $1.813*10^{-6}$). **c-d,** ET-Seq determined insertion efficiencies in the
104 nine-member consortium (n = 3 biological replicates) with conjugative delivery shown as **c,** a portion of the
105 entire community and **d,** a portion of each species. Control samples received no exogenous DNA. Average
106 relative abundances of community constituents across conjugation samples (n = 6 independent samples)
107 are indicated in parentheses. LOD and LOQ are indicated in plots by short and long dashed lines
108 respectively.
109
110 ET-Seq was developed and tested on a nine-member microbial consortium made up of
111 bacteria from three phyla that are often detected and play important metabolic roles within soil
112 microbial communities (Supplementary Table 1). We initially endeavored to test the accuracy and
113 detection limit by adding to the nine-member community a known amount of a previously prepared
114 *mariner* transposon library of one of its member species, *Klebsiella michiganensis* M5a1
115 (*Klebsiella_1*). The ET-Seq derived insertion efficiencies were closely correlated to the known
116 fractions of edited *K. michiganensis* present in each sample (Fig. 1b). Using this data we
117 calculated a limit of detection (LOD) and limit of quantification (LOQ) for our approach (Methods).
118 The LOD suggests that a fraction of $\geq 8.4*10^{-6}$ of transformed cells out of the total community
119 would be detectable by ET-Seq.
120 Next, the *mariner* transposon vector was delivered to the nine-member community through
121 conjugation. We could measure conjugation reproducibly and quantitatively in the three species
122 that grew to make up over 99% of the community (Fig. 1c). We further normalized insertion
123 efficiency in each species according to its abundance so that their insertion efficiencies represent
124 insertion containing cells as a portion of total cells for each species (Fig. 1d). Even for
125 *Paraburkholderia caledonica*, which made up ~0.1% of the community, we could measure
126 insertions. We detected no insertions in the remaining community members, which was expected
127 given their extreme rarity in the community (less than 0.05%).

128 We next used ET-Seq to compare insertion efficiencies in the nine-member community
129 after transposon delivery by conjugation, natural transformation with no induction of competence,
130 or electroporation of the transposon vector. Together these approaches showed reproducible
131 insertion efficiencies above the LOD in five of the nine community members (Fig. 2a and Extended
132 Data Fig. 2). Additionally we could identify preferred delivery methods for some members in this
133 community context, such as electroporation being consistently reproducible for *Dyella japonica*
134 *UNC79MFTsu3.2* while conjugation was not. These results show that ET-Seq can identify and
135 quantify genetic manipulation of microbial community members and reveal suitable DNA delivery
136 methods for each.
137

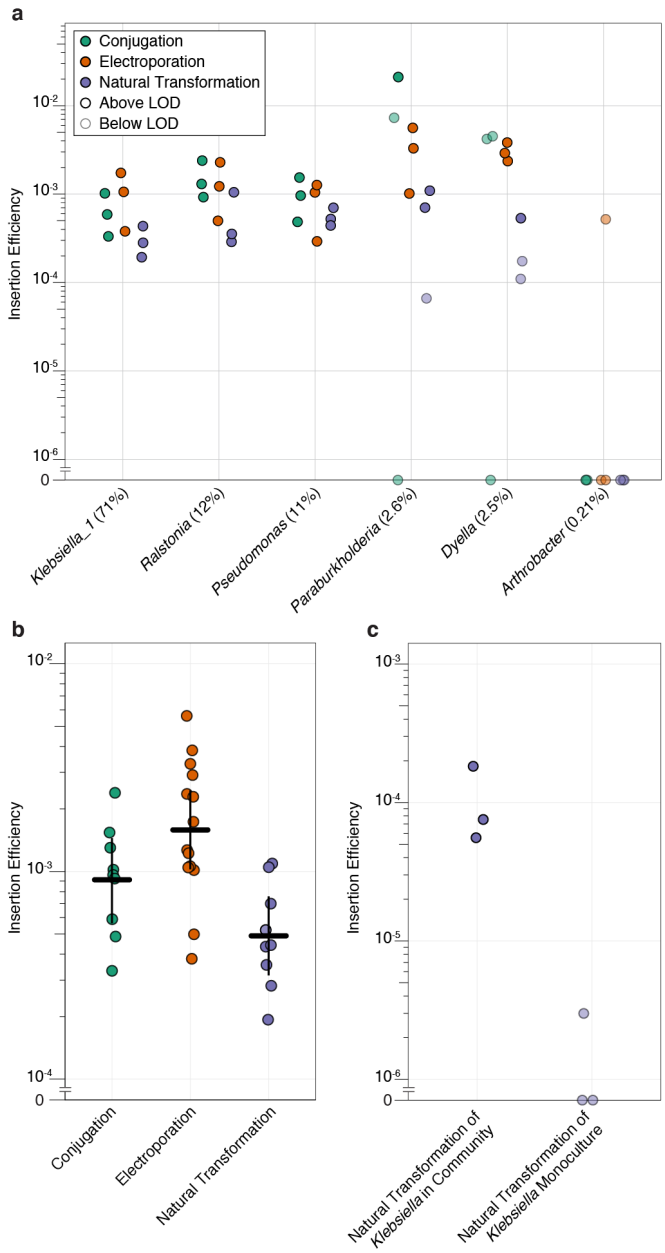

Fig. 2 | ET-Seq detection of insertion efficiency across multiple delivery approaches. a, ET-Seq determined insertion efficiencies for conjugation, electroporation, and natural transformation on the nine-member consortium (n = 3 biological replicates). Only members with at least one positive insertion efficiency value across the delivery methods are shown. Average relative abundance across all samples (n = 18 independent samples) is indicated in parentheses. **b,** Comparing delivery strategies across data from all organisms. Cross bars indicate the mean value and whiskers denote the 95% confidence interval for the mean (Conjugation n = 9; Electroporation n = 14; Natural Transformation n = 9). **c**, Comparison of insertion

146 efficiencies measured for natural transformation of *K. michiganensis* (*Klebsiella_1*) in isolated culture (n =
147 3 biological replicates) compared to *K. michiganensis* grown in the community context (n = 3 biological
148 replicates).
149
150 Notably, five organisms exhibited some degree of natural competency, although average
151 efficiencies were significantly lower for natural transformation than for delivery through
152 electroporation (ANOVA followed by Tukey's HSD; two-sided test; $p = 0.0009$) (Fig. 2b). To the
153 best of our knowledge, no isolates of the *Klebsiella* genus including *K. michiganensis* are known
154 to be naturally competent. We conducted a second experiment to compare the insertion efficiency
155 of *K. michiganensis* cultivated in isolation versus grown in the community context. ET-Seq
156 returned no values above the LOD for natural transformation of *K. michiganensis* in isolation, but
157 within the community ET-Seq returned values well into the quantifiable range (Fig. 2c). This
158 apparent emergent property of natural competence within a small synthetic community provides
159 tantalizing support for the possibility of community induced natural transformation, an idea suggested
160 in previous work, but experimentally unstudied due to lack of tools for measuring horizontal gene
161 transfer events within a community[13,14].
162
163 **Genetic accessibility of uncultivated species within an environmental microbiome**
164 To test the potential for editing in a complex and environmentally realistic community that has not
165 been reduced to isolates, we conducted ET-Seq on a genomically characterized 197 member
166 bioreactor-derived consortium that degrades thiocyanate (SCN^-), a toxic byproduct of gold
167 processing[15]. We sampled biofilm from the reactor and conducted ET-Seq with a panel of delivery
168 techniques: conjugation, electroporation, and natural transformation. Across ET-Seq replicates at
169 least one measurement above the LOD was identified for 15 members of the bioreactor
170 community. We also note that the transformed organisms make up ~87% of the bacterial fraction
171 by relative abundance (Fig. 3a, Extended Data Fig. 3). Ten of these organisms were species that

172 had not previously been isolated or edited (Supplementary Table 1), and overall members from 7
173 of the 12 phyla detected in this consortium were successfully transformed (Fig. 3b). This included
174 an *Afipia sp.* known to play an important role in the thiocyanate degradation process. Additionally,
175 one of the transposon recipients, *Microbacterium ginsengisoli* (*Microbacterium_3*), is a putative
176 host for Saccharibacteria, a candidate phyla radiation (CPR) organism that has been observed in
177 this reactor system[16]. Notably, members of the CPR are resistant to typical isolation techniques
178 due to heavy dependence on other community members, and little is known about the nature of
179 their likely symbiotic relationships with other organisms[17]. Here, ET-Seq has uncovered a
180 genetically tractable putative host organism, raising the possibility of genetically editing the host
181 to probe CPR/host symbiotic relationships within a complex microbial community. In this way, ET-
182 Seq reveals genetic accessibility and the tools necessary to achieve it in previously
183 unapproachable and biologically important members of an environmentally relevant community.

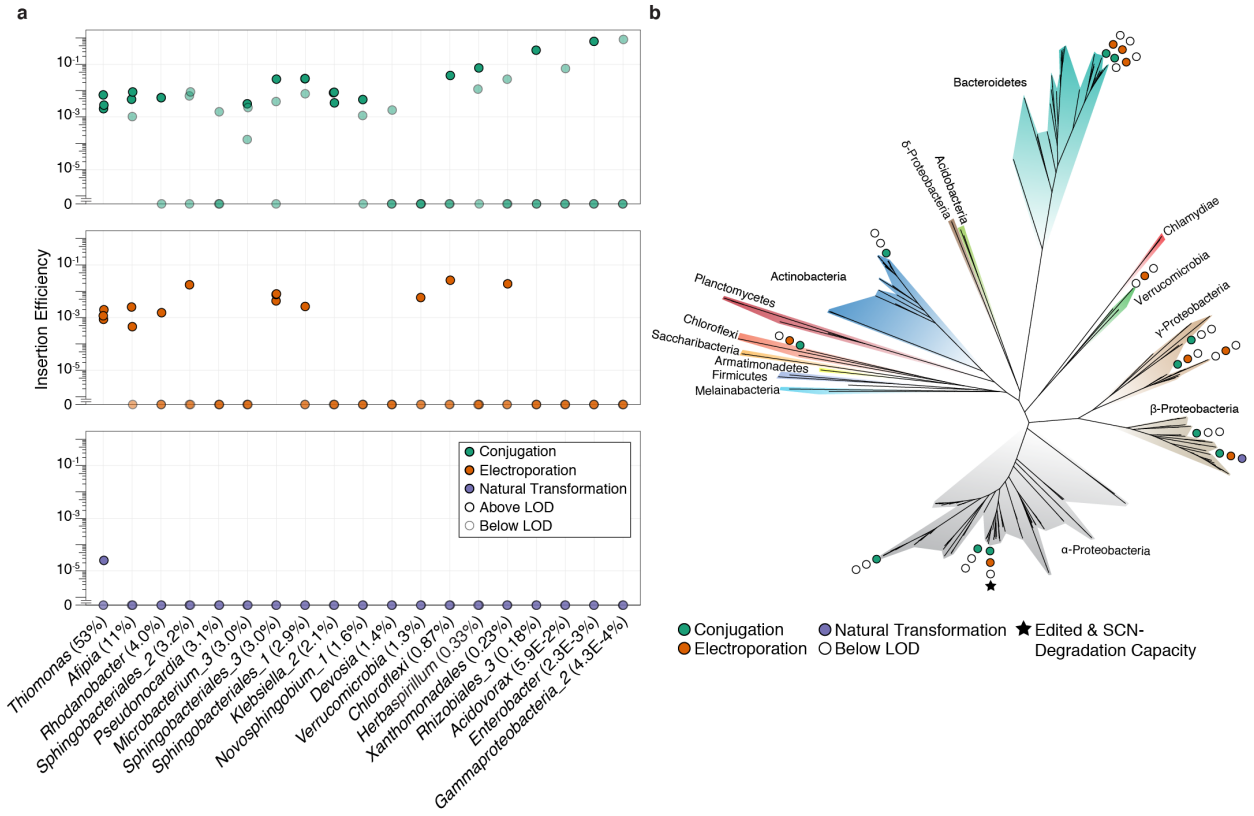

184

185 **Fig. 3 | ET-Seq detection of insertion efficiency in thiocyanate-degrading bioreactor. a,** ET-Seq

186 determined insertion efficiencies for conjugation, electroporation, and natural transformation on the
187 thiocyanate-degrading bioreactor community (n = 3 biological replicates). Average relative abundance
188 across all samples is indicated in parentheses (n = 17 independent samples). **b,** A ribosomal protein S3
189 (rpS3) phylogenetic tree of all organisms in the thiocyanate-degrading bioreactor genome database. Only
190 community members receiving at least one insertion by conjugation, electroporation, or natural
191 transformation detectable above LOD are indicated by filled circles. Filled circles indicate success of
192 method and open circles indicate method was not detected. A star indicates genomically encoded SCN^-
193 degradation capacity in organisms shown to be edited by at least one method. Tree was constructed from
194 an alignment of 262 rps3 protein sequences using IQ-TREE.
195

196 **Targeted genome editing in microbial communities using CRISPR-Cas transposases**

197 The ability to introduce genome edits to a single type of organism in a microbial community and
198 to target those edits to a defined location within its genome would be a foundational advance in
199 microbiological research and would have many useful applications. We reasoned that RNA-
200 guided CRISPR-Cas Tn7 transposases could provide the ability to both ablate function of targeted
201 genes and deliver customized genetic cargo in organisms shown to be genetically tractable by
202 ET-Seq[18–20] (Fig. 1a). However, the two-plasmid ShCasTn[18] and three-plasmid VcCasTn[19]
203 systems are not amenable to efficient delivery within complex microbial communities or even
204 beyond *E. coli* due to their multiple plasmids. Since ET-Seq identified conjugation and
205 electroporation as broadly effective delivery approaches in the tested communities, we designed
206 and constructed all-in-one conjugative versions of these CasTn vectors that could be used for
207 delivery by either strategy (Fig. 4a and Methods). These DART systems are barcoded and
208 compatible with the same sequencing methods used for ET-Seq, and can be used to assay the
209 efficacy of CRISPR-Cas-guided transposition into the genome of a target organism.
210

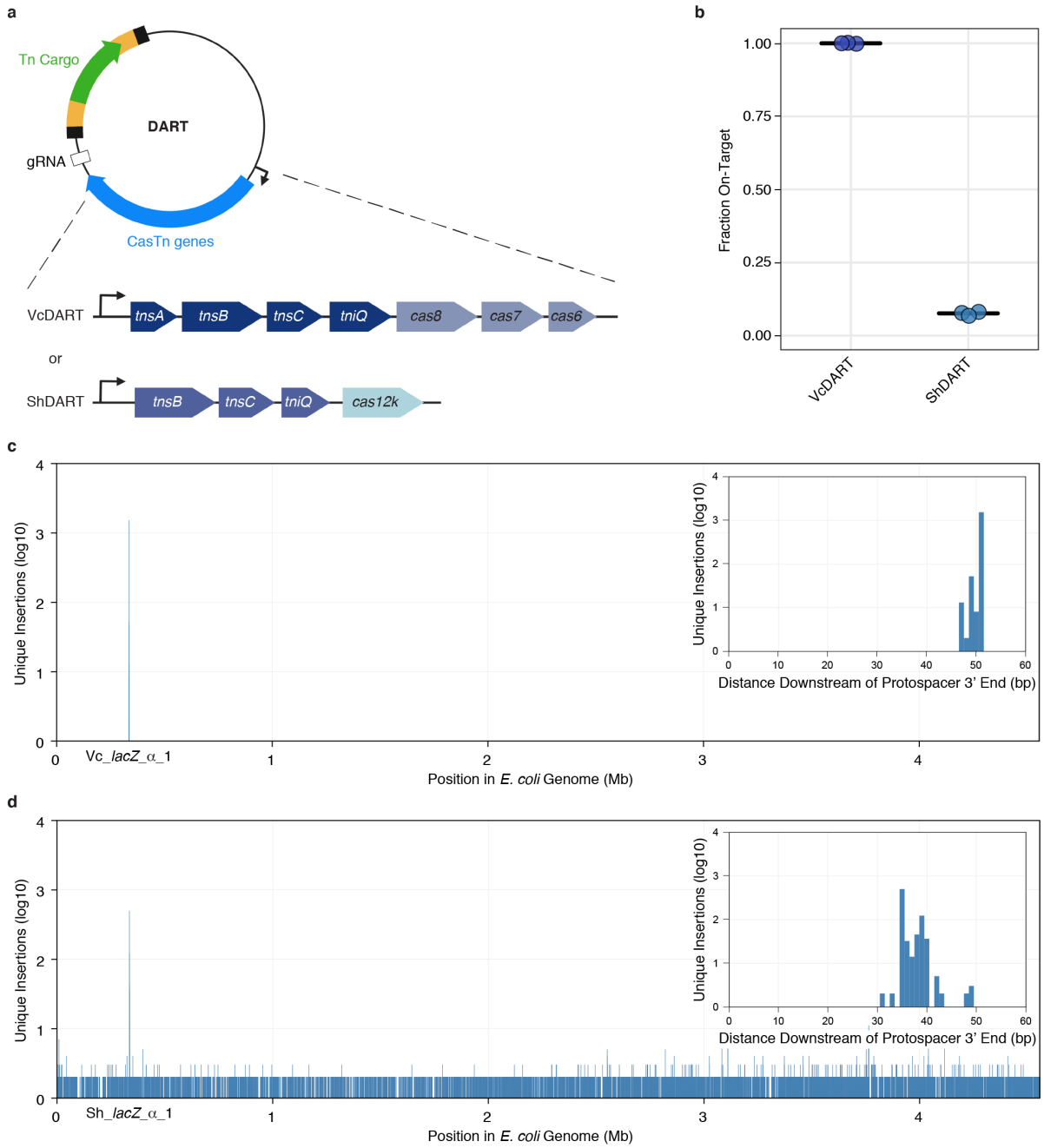

Fig. 4 | Benchmarking all-in-one conjugal targeted vectors. a, Schematic of VcDART and ShDART delivery vectors. **b,** Fraction of insertions that occur in a 60 bp window around the target site. Mean for three independent biological replicates is shown as cross bars. **c-d,** Aggregate unique insertion counts (n = 3 biological replicates) across the *E. coli* BL21(DE3) genome, determined by presence of unique barcodes, using **c,** VcDART and **d,** ShDART. The inset shows a 60 bp window downstream of the target site. Insertion distance downstream of the target site is calculated from the 3' end of the protospacer.

218

219 We compared the transposition efficiency and specificity of the DART systems in *E. coli*
220 in order to select the most promising candidate for targeted genome editing in microbial
221 communities. VcDART and ShDART systems harboring Gm^R cargo with a *lacZ*-targeting or non-
222 targeting guide RNA were conjugated into *E. coli* to quantify transposition efficiency, and target
223 site specificity was assayed using ET-Seq following outgrowth of transconjugants in selective
224 medium (Methods and Extended Data Fig. 4a). While ShDART yielded approximately tenfold
225 more colonies possessing insertions than ShDART (Extended Data Fig. 4), >92% of the
226 selectable colonies obtained using ShDART were off-target, compared to no detectable off-target
227 insertions for VcDART (Fig. 4b-d). Due to VcDART's high target site specificity and the
228 undesirable propensity for ShCasTn to co-integrate its donor plasmid[21,22], we focused on VcDART
229 to test the potential for targeted microbial community genome editing.

230

231 **Targeted microbial community editing by programmable transposition**

232 We reasoned that RNA-programmed transposition could be deployed for targeted editing of
233 specific types of organisms within a microbial consortium. ET-Seq had shown two species within
234 the nine-member community, *K. michiganesis* and *Pseudomonas simiae* WCS417, to be both
235 abundant and tractable by conjugation (Fig. 1d). We targeted both of these organisms using
236 conjugation to introduce the VcDART vector into the community with guide RNAs specific to their
237 genomes (Fig. 5a). Insertions were designed to produce loss-of-function mutations in the *K.*
238 *michiganesis* and *P. simiae pyrF* gene, an endogenous counterselectable marker allowing growth
239 in the presence of 5-fluoroorotic acid (5-FOA) when disrupted. The transposons carried two
240 antibiotic resistance markers conferring resistance to streptomycin and spectinomycin (*aadA*) and
241 carbenicillin (*bla*). Together the simultaneous loss-of-function and gain-of-function mutations
242 allowed for a strong selective regime. VcDART targeted to *K. michiganensis* or to *P. simiae pyrF*
243 followed by selection led to enrichment of these organisms to ~98% and ~97% pure culture

244 respectively (Fig. 5b). No outgrowth was detected when using a guide RNA that did not target
245 these respective microbial genomes. Recovered transformant colonies of *K. michiganensis* and
246 *P. simiae* analyzed by PCR and Sanger sequencing showed full length, *pyrF*-disrupting VcDART
247 transposon insertions 48-49 bp downstream of the guide RNA target site, consistent with
248 CRISPR-Cas transposase-catalyzed transposition events at the desired genomic location (Fig.
249 4c and 5c). These results demonstrate that targeted genome editing using DART enables genetic
250 manipulation of distinct members of a complex microbial community. This targeted editing of
251 microorganisms in a community context can also enable subsequent exploitation of modified
252 phenotypes.
253

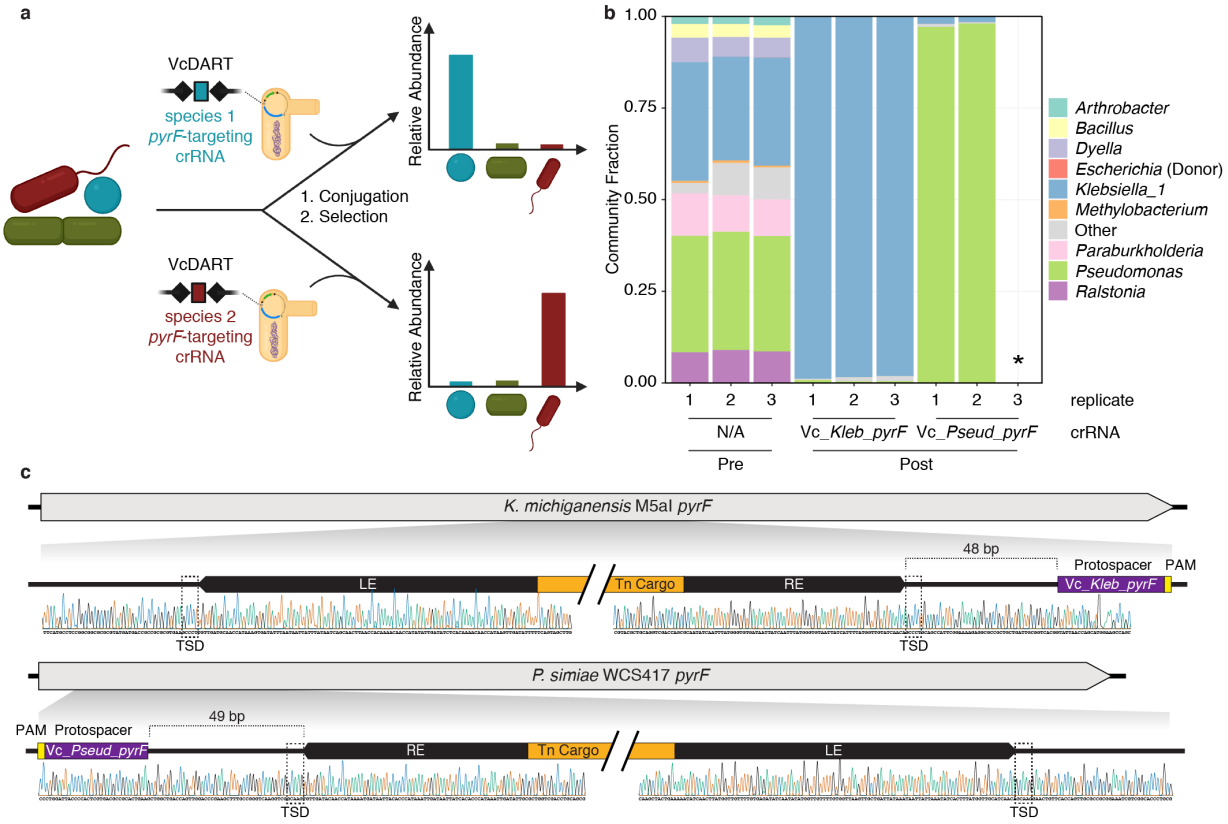

254

255 **Fig. 5 | Targeted editing in the nine-member consortium. a,** Conjugative VcDART delivery into a
256 microbial community using species-specific crRNA, followed by selection for transposon cargo, facilitates
257 selective enrichment of targeted organisms. **b,** Relative abundance of nine-member community

258 constituents measured by 16S rRNA sequencing before conjugative VcDART delivery and after selection
259 for *pyrF*-targeted transposition in *K. michiganensis* or *P. simiae* (n = 3 biological replicates). * indicates no
260 growth detected in selective medium. **c,** Representative Sanger sequencing chromatogram of PCR product
261 spanning transposon insertion site at targeted *pyrF* locus in *K. michiganensis* (top) and *P. simiae* (bottom)
262 colonies following VcDART-mediated transposon integration and selection. Target-site duplications (TSD)
263 are indicated with dashed boxes.
264

265 **Discussion**

266 We have demonstrated organism- and locus-specific genome editing within a microbial
267 community, providing a new approach to microbial genetics and microbiome manipulation for
268 research and applications. ET-Seq revealed the genetic accessibility of organisms growing within
269 microbial communities, including ten microbial species that had not been previously isolated or
270 found to be genetically manipulated. The creation of all-in-one vectors encoding two naturally
271 occurring CRISPR-Cas transposon systems enabled comparison of their targeted genome editing
272 capabilities. These experiments showed that only one of the two systems, which we termed
273 VcDART, enabled precise RNA-programmable microbial genome editing. The ability to conduct
274 targeted genome editing of two bacteria within a nine-member synthetic community and to use
275 the introduced genetic changes as a means of organism isolation demonstrates a new approach
276 to microbiome manipulation. Traditionally, the combined steps of culturing an environmental
277 microbe, determining the ideal means to transform it, and implementing targeted editing could
278 take years or could fail altogether[23]. ET-Seq combined with VcDART compresses the pipeline for
279 establishing genetics in microorganisms to weeks and expands the diversity of organisms that
280 can be targeted beyond those that can be cultivated in isolation.

281 In addition to providing a roadmap for targeted microbial genome editing, ET-Seq can be
282 used to discover and analyze horizontal gene transfer in complex communities. In this study, we
283 observed unexpected community-dependent natural transformation in the nine-member

284 community and characterized the horizontal gene transfer events experimentally in the complex
285 microbiome of a thiocyanate-degrading bioreactor. In future experiments, multiple ET-Seq time
286 points could be taken in a community after delivery to measure directly both the portion of the
287 community receiving DNA and the persistence of gene transfer, rather than tracking horizontal
288 gene transfer using bioinformatics[24] or indirect experimental methods[4–9]. Furthermore, as ET-Seq
289 is applied in increasingly diverse and complex environments, an atlas of editable taxa can be
290 created including optimal delivery approaches. To expand this dataset, we plan to apply ET-Seq
291 to new microbial communities being sampled for metagenomic sequencing, a natural pairing
292 because ET-Seq depends on availability of genome sequences for the component organisms.

293 In the future, tools are needed to create more generally applicable and persistent targeted
294 genome edits. The canonical approach involving antibiotic selection for edited bacteria is
295 infeasible in large complex communities, where many natural resistances exist[25,26]. Even in the
296 nine-member synthetic community used in this study, three antibiotics and counterselection were
297 necessary to achieve strict selection. Improved delivery strategies and alternative positive and
298 counter selection methods should enable more efficient editing. In the gut microbiome, porphyran
299 has been used successfully for selection of a spiked-in organism capable of utilizing this
300 compound[27]. Such approaches for more efficient microbial community editing will enable research
301 to answer fundamental questions as well as allow manipulation of agricultural, industrial, and
302 health-relevant microbiomes. The combination of ET-Seq and DART systems presented here
303 provide the foundation of the new field of *in situ* microbial genetics.

304

305 **References**

306 1. Steen, A. D. *et al.* High proportions of bacteria and archaea across most biomes remain
307 uncultured. *ISME J.* (2019) doi:10.1038/s41396-019-0484-y.

308 2. Pascual-García, A., Bonhoeffer, S. & Bell, T. Metabolically cohesive microbial consortia and

309 ecosystem functioning. *Philos. Trans. R. Soc. Lond. B Biol. Sci.* **375**, 20190245 (2020).
310 3. Fux, C. A., Shirtliff, M., Stoodley, P. & Costerton, J. W. Can laboratory reference strains
311 mirror 'real-world' pathogenesis? *Trends Microbiol.* **13**, 58–63 (2005).
312 4. Pukall, R., Tschäpe, H. & Smalla, K. Monitoring the spread of broad host and narrow host
313 range plasmids in soil microcosms. *FEMS Microbiol. Ecol.* **20**, 53–66 (1996).
314 5. De Gelder, L., Vandecasteele, F. P. J., Brown, C. J., Forney, L. J. & Top, E. M. Plasmid
315 Donor Affects Host Range of Promiscuous IncP-1β Plasmid pB10 in an Activated-Sludge
316 Microbial Community. *Appl. Environ. Microbiol.* **71**, 5309–5317 (2005).
317 6. Musovic, S., Oregaard, G., Kroer, N. & Sørensen, S. J. Cultivation-Independent
318 Examination of Horizontal Transfer and Host Range of an IncP-1 Plasmid among Gram-
319 Positive and Gram-Negative Bacteria Indigenous to the Barley Rhizosphere. *Applied and*
320 *Environmental Microbiology* vol. 72 6687–6692 (2006).
321 7. Musovic, S., Klümper, U., Dechesne, A., Magid, J. & Smets, B. F. Long-term manure
322 exposure increases soil bacterial community potential for plasmid uptake. *Environ.*
323 *Microbiol. Rep.* **6**, 125–130 (2014).
324 8. Klümper, U. *et al.* Broad host range plasmids can invade an unexpectedly diverse fraction
325 of a soil bacterial community. *ISME J.* **9**, 934–945 (2015).
326 9. Ronda, C., Chen, S. P., Cabral, V., Yaung, S. J. & Wang, H. H. Metagenomic engineering
327 of the mammalian gut microbiome in situ. *Nat. Methods* **16**, 167–170 (2019).
328 10. Farzadfard, F., Gharaei, N., Citorik, R. J. & Lu, T. K. Efficient Retroelement-Mediated DNA
329 Writing in Bacteria. *bioRxiv* (2020).
330 11. Hsu, B. B., Way, J. C. & Silver, P. A. Stable Neutralization of a Virulence Factor in Bacteria
331 Using Temperate Phage in the Mammalian Gut. *mSystems* **5**, (2020).
332 12. Sheth, R. U., Cabral, V., Chen, S. P. & Wang, H. H. Manipulating Bacterial Communities by
333 in situ Microbiome Engineering. *Trends Genet.* **32**, 189–200 (2016).
334 13. Wang, X. *et al.* Across Genus Plasmid Transformation Between Bacillus subtilis and

335 Escherichia coli and the Effect of Escherichia coli on the Transforming Ability of Free
336 Plasmid DNA. *Current Microbiology* vol. 54 450–456 (2007).
337 14. Borgeaud, S., Metzger, L. C., Scrignari, T. & Blokesch, M. The type VI secretion system of
338 Vibrio cholerae fosters horizontal gene transfer. *Science* **347**, 63–67 (2015).
339 15. Kantor, R. S. *et al.* Genome-Resolved Meta-Omics Ties Microbial Dynamics to Process
340 Performance in Biotechnology for Thiocyanate Degradation. *Environ. Sci. Technol.* **51**,
341 2944–2953 (2017).
342 16. Huddy, R. J. *et al.* Thiocyanate and organic carbon inputs drive convergent selection for
343 specific autotrophic Afipia and Thiobacillus strains within complex microbiomes. *bioRxiv*
344 2020.04.29.067207 (2020) doi:10.1101/2020.04.29.067207.
345 17. Castelle, C. J. *et al.* Biosynthetic capacity, metabolic variety and unusual biology in the
346 CPR and DPANN radiations. *Nat. Rev. Microbiol.* **16**, 629–645 (2018).
347 18. Strecker, J. *et al.* RNA-guided DNA insertion with CRISPR-associated transposases.
348 *Science* **365**, 48–53 (2019).
349 19. Klompe, S. E., Vo, P. L. H., Halpin-Healy, T. S. & Sternberg, S. H. Transposon-encoded
350 CRISPR–Cas systems direct RNA-guided DNA integration. *Nature* **571**, 219–225 (2019).
351 20. Petassi, M. T., Hsieh, S.-C. & Peters, J. E. Guide RNA categorization enables target site
352 choice in Tn7-CRISPR-Cas transposons. *bioRxiv* 2020.07.02.184150 (2020)
353 doi:10.1101/2020.07.02.184150.
354 21. Rice, P. A., Craig, N. L. & Dyda, F. Comment on 'RNA-guided DNA insertion with CRISPR-
355 associated transposases'. *Science* **368**, (2020).
356 22. Strecker, J., Ladha, A., Makarova, K. S., Koonin, E. V. & Zhang, F. Response to Comment
357 on 'RNA-guided DNA insertion with CRISPR-associated transposases'. *Science* **368**,
358 (2020).
359 23. Laurenceau, R. *et al.* Toward a genetic system in the marine cyanobacterium
360 Prochlorococcus. *Access Microbiology* **6**, 23 (2020).

361 24. Soucy, S. M., Huang, J. & Gogarten, J. P. Horizontal gene transfer: building the web of life.
362 *Nat. Rev. Genet.* **16**, 472–482 (2015).
363 25. Hu, Y. *et al.* Metagenome-wide analysis of antibiotic resistance genes in a large cohort of
364 human gut microbiota. *Nat. Commun.* **4**, 2151 (2013).
365 26. Forsberg, K. J. *et al.* Bacterial phylogeny structures soil resistomes across habitats. *Nature*
366 **509**, 612–616 (2014).
367 27. Shepherd, E. S., DeLoache, W. C., Pruss, K. M., Whitaker, W. R. & Sonnenburg, J. L. An
368 exclusive metabolic niche enables strain engraftment in the gut microbiota. *Nature* **557**,
369 434–438 (2018).

370

371 **Methods**

372 **Plasmid construction and barcoding**

373 For ET-Seq measurement of genetic tractability in community members, DNA encoding a non-
374 targeted *mariner* transposon was delivered. The *mariner* transposon integrates into "TA"
375 sequences in recipient cells. For delivery of the *mariner* transposon, we made use of the
376 previously created pHLL250 vector, which contains an RP4 origin of transfer (oriT), AmpR,
377 conditional (*pir*$^{+}$-dependent) R6K origin, and an AseI restriction site to facilitate depletion of vector
378 from DNA samples in ET-Seq library preparations[1]. Unique to each transposon on this vector is
379 a random 20 bp barcode sequence to aid in the discrimination of unique insertion events from
380 duplications of the same insertion due to cell division or PCR.

381 DART vectors were designed to encode all components required for delivery and editing
382 (Supplementary Table 2 and Extended Data Fig. 4). VcCasTn genes, crRNA, and Tn were
383 synthesized as gBlocks (IDT). pHelper_ShCAST_sgRNA was a gift from Feng Zhang (Addgene
384 plasmid #127921; http://n2t.net/addgene:127921; RRID:Addgene_127921) and was used to
385 clone ShCasTn genes and sgRNA. pDonor_ShCAST_kanR was a gift from Feng Zhang
386 (Addgene plasmid # 127924 ; http://n2t.net/addgene:127924 ; RRID:Addgene_127924) and was
387 used to clone the ShCasTn transposon. *tns* genes, *cas* genes, and crRNA/sgRNA were
388 consolidated into a single operon (with various promoters and transcriptional configurations) on
389 the same vector as the cognate transposon. The left end of the cognate Tn was encoded
390 downstream of the crRNA/sgRNA, followed by Tn cargo, barcode, and Tn right end. DART Tn LE
391 and RE were designed to include the minimal sequence that both included all putative TnsB
392 binding sites and was previously shown to be functional[2,3]. Specifically, VcDART LE (108 bp) and
393 RE (71 bp) each encompass three 20 bp putative TnsB binding sites, spanning from the edge of
394 the 8 bp terminal ends to the edge of the third putative TnsB binding site[2]. ShDART LE (113 bp)
395 spans the boundaries of the long terminal repeat and both additional putative TnsB binding sites,

396 while the RE (211 bp) encompasses the long terminal repeat and all four additional putative TnsB
397 binding sites[3].
398 Vectors were cloned using BbsI (NEB) Golden Gate assembly of part plasmids, each
399 encoding different regions of the final plasmid. Of note, the backbone encodes RP4 oriT, AmpR,
400 conditional R6K origin, and an AsiSI+SbfI double digestion site for vector depletion during ET-
401 Seq library preparations. A 2xBsaI spacer placeholder enabled spacer cloning with BsaI (NEB)
402 Golden Gate. A 2xBsmBI barcode placeholder was encoded immediately inside the Tn right end
403 and was used for barcoding as described below. Part plasmids were propagated in *E. coli* Mach1-
404 T1R (QB3 Macro Lab). Golden Gate reactions for all-in-one vector assembly were purified with
405 DNA Clean & Concentrator-5 (Zymo Research) and electroporated into *E. coli* EC100D-*pir*+
406 (Lucigen).
407 DART vectors were barcoded by BsmBI (NEB) Golden Gate insertion of random barcode
408 PCR product into the 2xBsmBI barcode placeholder using a previously reported method[4] with
409 slight modifications. A 56-nt ssDNA oligonucleotide encoding a central tract of 20 degenerate
410 nucleotides (oBFC1397) was amplified with BsmBI-encoding primers oBFC1398 and oBFC1399
411 using Q5 High-Fidelity 2X Master Mix (NEB) in a six-cycle PCR (98°C for 1 min; six cycles of 98°C
412 for 10 s, 58°C for 30 s, and 72°C for 60 s; and 72°C for 5 min). Barcoding Golden Gate reactions
413 were purified with DNA Clean & Concentrator-5. To remove residual non-barcoded vector,
414 reactions were digested with 15 U BsmBI at 55°C for at least 4 hr, heat inactivated at 80°C for 20
415 min, treated with 10 U Plasmid-Safe ATP-Dependent DNase (Lucigen) exonuclease at 37°C for
416 1 hr, heat inactivated at 70°C for 30 min, and purified with DNA Clean & Concentrator-5.
417 Randomly barcoded conjugative vectors were electroporated into *E. coli* EC100D-*pir*+,
418 followed 1 hr recovery in 1 mL pre-warmed SOC (NEB) at 37°C 250 rpm, serial dilution and spot
419 plating on LB agar plus 100 µg mL^{-1} carbenicillin to estimate library diversity, and plating the full
420 transformation across 5 LB agar plates containing carbenicillin (and other appropriate antibiotics
421 when Tn cargo contained other resistance cassettes). To prepare barcoded conjugative vector

422 plasmid stock, all 5 agar plates were scraped into a single pool and midiprepped (Zymo
423 Research). All conjugations were performed using the diaminopimelic acid (DAP) auxotrophic
424 RP4 conjugal donor *E. coli* strain WM3064. Donor strains were prepared by electroporation with
425 200 ng barcoded vectors, followed by recovery in SOC plus DAP at 37°C and 250 rpm and
426 inoculation of the entire recovery culture into 15 mL LB containing DAP and carbenicillin in 50 mL
427 conical tubes, followed by overnight cultivation at 37°C and 250 rpm. Donor serial dilutions were
428 spot plated on LB agar plus carbenicillin to estimate final barcode diversity.
429
430 **Guide RNA design**
431 In all experiments, VcCasTn gRNAs used 32 nt spacers and a 5'-CC Type IF PAM, while
432 ShCasTn gRNAs used 23 nt spacers and a 5'-GTT Cas12k PAM. All gRNAs were designed to
433 bind in the first half of the target CDS to ensure functional knockout by transposon insertion
434 (Supplementary Table 3). Off-target potential was assessed using BLASTn (-dust no -word_size
435 4) of spacers against a local BLAST database created from all genomes present in an experiment,
436 and spacers were discarded if off-target hits with E-value < 15 were identified. gRNAs with less
437 seed region complementarity to off-targets were prioritized. Non-targeting gRNAs were designed
438 by scrambling the spacer until no significant matches were found.
439
440 **Delivery methods**
441 For natural transformation and electroporation, a culture of the community or isolate to be
442 transformed was subcultured at OD_{600} = 0.2 and grown to OD_{600} = 0.5. In the case of the
443 thiocyanate-degrading bioreactor in the absence of accurate OD measurements the culture was
444 outgrown for two hours. For natural transformation 200 ng of vector harboring the *mariner*
445 transposon (pHLL250[1]) for non-targeted insertion, or water for the negative control were added
446 to 4 mL of OD_{600} = 0.5 outgrowth. Cultures were incubated for 3 hours shaking at 250 rpm at

447 temperature appropriate for the isolate or community before being moved to the appropriate
448 downstream analysis.

449 For electroporation, 20 mL of the community or isolate at OD_{600} = 0.5 was put on ice,
450 centrifuged at 4,000*g* at 4°C for 10 minutes, and washed four times with 10 mL sterile ice-cold
451 Milli-Q H_2O. After a final centrifugation the pellet was resuspended in 100 µL of 2 ng/µL vector
452 (pHLL250 or VcDART), or 100 µL of water as a negative control. This solution was then pipetted
453 into a 0.2 cm gap ice-cold cuvette and electroporated at 3 kV, 200Ω, and 25 µF. The cells were
454 immediately recovered into 10 mL of the community's or isolate's preferred medium and incubated
455 shaking for 3 hours before being moved to the appropriate downstream analysis.

456 *E. coli* strain WM3064 containing the *mariner* transposon (pHLL250) for non-targeted
457 editing, or the VcDART for targeted editing was cultured overnight in LB supplemented with
458 carbenicillin (100 µg/mL) and DAP (60 µg/mL) at 37°C. Before conjugation the donor strain was
459 washed twice in LB (centrifugation at 4,000*g* for 10 minutes) to remove antibiotics. Then, 1
460 OD_{600}*mL of the donor was added to 1 OD_{600}*mL of the recipient community or isolate and the
461 mixture was plated on a 0.45 µm mixed cellulose ester membrane (Millipore) topping a plate of
462 the recipient's preferred media without DAP. In the case of the thiocyanate-degrading bioreactor,
463 ~2 OD_{600}*mL of the donor was added to 2 OD_{600}*mL of the recipient community to ensure
464 sufficient material despite the community's slow growth. Plates were incubated at the ideal
465 temperature for the recipient community or isolate for 12 hours before the growth was scraped off
466 the filter into the media of the recipient community or isolate for downstream analysis.

467

468 **ET-Seq library preparation**

469 The insertion junction sequencing library prep strategy for ET-Seq can be used (modification may
470 be necessary) in any circumstance where high efficiency mapping of inserted DNA to a host loci
471 is desired. For our purposes, DNA of the edited community or isolate was first extracted using

472 the DNeasy PowerSoil Kit (QIAGEN). In the case of the nine-member community, 500 ng of DNA
473 was used for both insertion junction sequencing and metagenomic library prep. For the SCN
474 community, which had lower yields of DNA, 100 ng were used . As an internal standard, DNA
475 from a previously constructed mutant library of *Bacteroides thetaiotaomicron* VPI-5482[5], a
476 species not present in the nine-member community or the thiocyanate-degrading bioreactor, was
477 spiked into the community DNA at a ratio of 1/500 by mass. The *B. thetaiotaomicron* library had
478 undergone antibiotic selection for its transposon insertions and was thus assumed to represent
479 100% transformation efficiency (i.e. every genome contained at least one mariner transposon
480 insertion).

481 For metagenomic sequencing, library prep was conducted by the standard ≥100 ng
482 protocol from the NEBNext Ultra II FS DNA Library Prep Kit for Illumina (NEB). For insertion
483 junction sequencing, the same protocol was used with a number of modifications enumerated
484 here (Extended Data Fig. 1). This insertion junction sequencing protocol has also been tested
485 successfully with the ≤ 100 ng protocol of the NEBNext Ultra II FS DNA Library Prep Kit (NEB)
486 and the KAPA HyperPlus Kit (Roche). For fragmentation an 8 minute incubation was used. A
487 custom splinklerette adaptor was used during adaptor ligation to decrease non-specific
488 amplification (Supplementary Table 4)[6,7]. For size selection 0.15X (by volume) SPRIselect
489 (Beckman Coulter, Cat # B23318) or NEBNext Sample Purification Beads (NEB) were used for
490 the first bead selection and 0.15X (by volume) were added for the second. From this selection,
491 the DNA was eluted in 44 µL (instead of the suggested 15 µL) where it undergoes digestion before
492 enrichment to cleave intact transposon delivery vector. All bead elutions were performed with
493 Sigma Nuclease-Free water. pHLL250 underwent AseI digestion, while DART vectors underwent
494 double digestion by AsiSI and SbfI-HF (NEB) (Supplementary Table 2). The DNA then underwent
495 a sample purification using 1X AMPure XP beads (Beckman Coulter) to prepare it for PCR
496 enrichment.

497 In PCR enrichment, the transposon junction was amplified by nested PCR. The PCRs
498 followed the NEBNext Ultra II FS DNA Library Prep Kit for Illumina (NEB) PCR protocol, however
499 in the first PCR the primers were custom to the transposon and the adaptor and the PCR was run
500 for 25 cycles (Supplementary Table 4). The enrichment then underwent sample purification with
501 a 0.7X size selection using SPRIselect or NEBNextSample Purification Beads from which 15 µL
502 were eluted for the second PCR. This second PCR used custom unique dual indexing primers
503 specific to nested regions of the insertion and adaptor and 6 cycles are used (Supplementary
504 Table 4). Then another 0.7x size selection was conducted and the final library was eluted in 30
505 µL. Samples for metagenomic sequencing and insertion junction sequencing were then quality
506 controlled and multiplexed using 1X HS dsDNA Qubit (Thermo Fisher) for total sample
507 quantification, Bioanalyzer DNA 12000 chip (Agilent) for sizing, and qPCR (KAPA) for
508 quantification of sequenceable fragments. Samples were sequenced on the iSeq100 or
509 HiSeq4000 platforms.
510
511 **Genome sequencing, assembly, taxonomic classification, and database construction**
512 For a full list of genome sequences used as read mapping references in this study see
513 Supplementary Table 1. Assembly and annotation of genomes used as references for the SCN
514 bioreactor experiment is described in Huddy et al.[8]. As the SCN bioreactor has been subjected to
515 numerous genome-resolved metagenomic studies[8,9] we endeavored to create a non-redundant
516 database that contained all genomes previously observed in this reactor system. A set of 556
517 genomes assembled from this system were de-replicated at the species level using dRep v2.5.3[10]
518 with an average nucleotide identity (ANI) threshold of 95% and a minimum completeness of 60%
519 as estimated by checkM v1.1.2[11]. A single genome representing each species level group was
520 chosen by dRep based on optimizing genome size, fragmentation, estimated completeness, and
521 estimated contamination resulting in 265 representative genomes. Genomes were taxonomically
522 classified using GTDB-Tk[12] with default options. Additionally, to display the taxonomic diversity of

523 transformed organisms (Fig. 3b), a phylogenetic tree was constructed using ribosomal protein S3
524 (rpS3). Briefly, a custom Hidden Markov Model (HMM) was used to identify rpS3 sequences[13] in
525 the 265 representative genomes, and 262 rpS3 sequences were successfully identified.
526 Sequences were aligned using muscle[14], and a maximum likelihood phylogenetic tree was
527 constructed using IQ-TREE[15]. Phylogenetic trees were pruned and annotated using iTol v5
528 (https://itol.embl.de/). To determine if an organism we identified as receiving exogenous DNA was
529 ever previously isolated we used the ANI relative to the closest reference genome in the GTDB-
530 Tk output. If one of our genomes had an ANI ≥ 95% relative to a known reference, and this
531 reference genome was generated from an isolated bacterium, our target organism was
532 considered to be previously isolated (Supplementary Table 1).

533 For 9-member community genomes assembled as part of this study, cultures were grown
534 on R2A medium for 24 hours at 30°C and genomic DNA was extracted with the DNeasy Blood
535 and Tissue DNA Kit (Qiagen) with pre-treatment for Gram-positive bacteria. Genomic DNA was
536 sheared mechanically with the Covaris S220 and processed with the NEBNext DNA Library Prep
537 Master Mix Set for Illumina (NEB) before submitting for sequencing on an Illumina MiSeq platform
538 generating paired end 150 bp reads. Raw sequencing reads were processed to remove Illumina
539 adapter and phiX sequence using BBduk with default parameters, and quality trimmed at 3' ends
540 with Sickle using default parameters (https://github.com/najoshi/sickle). Assemblies were
541 conducted using IDBA-UD v1.1.1[16] with the following parameters: –pre_correction –mink 30 –
542 maxk 140 –step 10. Following assembly, contigs smaller than 1 kbp were removed and open
543 reading frames (ORFs) were then predicted on all contigs using Prodigal v2.6.3[17]. 16S ribosomal
544 rRNA genes were predicted using the 16SfromHMM.py script from the ctbBio python package
545 using default parameters (https://github.com/christophertbrown/bioscripts). Transfer RNAs were
546 predicted using tRNAscan-SE[18]. The full metagenome samples and their annotations were then
547 uploaded into our in-house analysis platform, ggKbase, where genomes were manually curated

548 via the removal of contaminating contigs based on aberrant phylogenetic signatures
549 (https://ggkbase.berkeley.edu).
550 For each ET-Seq experiment a genomic database is constructed using the ETdb
551 component of the ETsuite software package. Each database contains the nucleotide sequences
552 of the expected organisms in a sample, any vectors used, any conjugal donor, and the spike in
553 control organism. Briefly, all genomic sequences are formatted into a bowtie2 index to allow read
554 mapping, a tabular correspondence table between all scaffold names and their associated
555 genome is constructed (scaff2bin.txt), and a table (genome_info.txt) of standard genomic
556 statistics is calculated including genome size, GC content, and number of scaffolds. Following
557 database construction, a label is manually added to each entry in the genome info table to indicate
558 if the entry represents a target organism, a vector, or a spike in control organism. All data are
559 propagated into a single folder that can be used by the ETmapper software for downstream
560 mapping and analysis.
561
562 **Identification and quantification of insertion junctions and barcodes**
563 To identify and map transposon insertion junctions and their associated barcodes in a mixed
564 population of microbial cells, reads (150 bp X 2) generated from PCR amplicons of putative
565 transposon insertion junctions are first processed using the ETmapper component of the ETsuite
566 software package implemented in R with the following steps: First reads are quality trimmed at
567 the 3' end to remove low quality bases (Phred score ≤ 20) and sequencing adapters using
568 Cutadapt v2.10[19]. Cutadapt is then used to identify and remove provided transposon model
569 sequences from the 5' end of forward reads, requiring a match to 95% of the shortest transposon
570 sequence in a provided set and allowing a 2% error rate. Read pairs where no transposon model
571 sequence is identified in the forward read are discarded. All identified and trimmed transposon
572 models are paired with their respective reads, stored, and barcodes are identified in these
573 sequences by searching for a known primer binding site sequence flanking the 5' end of the

574 barcode (5'-CTATAGGGGATAGATGTCCACGAGGTCTCT-3') allowing for 1 mismatch.
575 Subsequently, the 20 bp region following the known primer binding site is extracted as the barcode
576 sequence and associated with its respective read. The 3' end of the paired reverse reads are then
577 trimmed to remove any transposon model sequence using Cutadapt, and only read pairs where
578 one mate is at least ≥ 40 bp following all trimming are retained for downstream mapping and
579 analysis. The fully trimmed paired end reads now consisting of only genomic sequence following
580 the transposon insertion site are mapped to the ETdb database used in a given experiment using
581 bowtie2 with default options[20]. Mapped read files are converted into a hit table indicating the
582 mapped genome, scaffold, genomic coordinates, mapQ score, and number of alignment
583 mismatches for each read in a pair using a custom Python script, bam_pe_stats.py, provided with
584 ETsuite. This table is then merged with read-barcode assignments to generate a final hit table
585 with the mapping information about each read pair, the transposon model identified, and the
586 associated barcode found for that read pair. Finally mapped read pairs are only retained for
587 downstream quantification if both reads map to the same genome, at least one mapped read in a
588 pair has a mapQ score ≥ 20, and a barcode was successfully identified and associated with the
589 read pair.

590 To quantify the number of unique barcodes and their associated reads mapping to
591 organisms in each sample of an experimental run, the filtered hit tables were processed using the
592 ETstats component of the ET-Seq software package with the following steps: Initially, all barcodes
593 identified across all samples in an experiment are aggregated and clustered using Bartender[21]
594 with the following supplied options: -l 4 -s 1 -d 3. Barcode clusters and their associated
595 barcodes/reads were only retained if all of the following criteria were true: (1) ≥ 75% of the reads
596 in a cluster mapped to one genome (the majority genome), (2) ≥ 75% of the reads in a cluster
597 were associated with the same transposon model (the majority model), and (3) the barcode
598 cluster had at least 2 reads. Subsequently, when quantifying reads and barcodes in each sample
599 of an experiment, the genome a read was mapped to and the transposon model it was associated

600 with had to agree with the majority assignments for the barcode cluster assigned to that read's
601 barcode to be counted. Finally, we were aware that Illumina patterned flow cell related index
602 swapping would result in reads from a barcode cluster being misassigned across samples, even
603 when using unique dual indexing[22]. We could not simply limit barcode clusters to be associated
604 with only one sample, as our spike in control organisms contain the same pool of barcodes and
605 are added to every sample. Thus we estimated an empirical index swap rate across each
606 experiment and required that the number of reads (X) for a barcode to be positively identified in
607 a sample be always ≥ 2 and ≥ the binomial mean of observed read counts expected in any sample
608 for a barcode cluster with (R) reads across (N) samples based on the estimated swap rate (S) +
609 2 standard deviations (**Eqn. 1**)
610
611 **Eqn. 1:** $X \geq \left(R \times \left(\frac{S}{N}\right)\right) + 2 \times \sqrt{R \times (1 - S) \times S} \ \ \& \ \ X \geq 2$
612
613 The index swap rate for an experiment was empirically estimated from barcode clusters assigned
614 only to target organisms based on the assumption that it would be highly unlikely for a barcode
615 cluster to have truly originated from independent integration events into the same organism in
616 more than one sample. Thus we assumed that for each barcode cluster associated with target
617 organisms, the majority of reads originated from the true sample and reads assigned to other
618 samples represented swaps. This is opposed to barcode clusters associated with our spike-in
619 organism, conjugal donor organism, or vectors which contain the same pool of barcodes directly
620 added to multiple samples. To identify swapped read counts we first quantify the total count of all
621 reads assigned to the majority genome across barcode clusters but that are not associated with
622 the majority sample of that cluster (E). Then we quantify the total count of reads associated with
623 the majority genome and associated with the majority sample across all clusters (C). Then

experiment wide swap rate was estimated by dividing the total number of reads not associated with majority samples by the total number of reads (**Eqn. 2**)

Eqn. 2: $S = \frac{E}{(E + C)}$

Following filtering, a hit table is returned that indicates for each genome in each sample, the number of unique barcode clusters that were recovered, and the total number of reads associated with these barcodes. As a final check for false positives during ET-Seq development we included an organism genome as an ETsuite mapping target, *Sinorhizobium meliloti*, which was not physically included in our 9-member synthetic or thiocyanate-degrading communities. We did not detect any barcodes or reads associated with this genome.

Metagenomic data processing and coverage calculation.

Each ET-Seq sample is split and in parallel undergoes shotgun metagenomic sequencing to determine the relative quantities of organisms present in the sample at the time of sampling. Raw read files from metagenomic data are also processed using the ETmapper component of the ETsuite software package with the following steps: First reads are quality trimmed at the 3' end to remove low quality bases (Phred score ≤ 20) and sequencing adapters using Cutadapt v2.10[19]. Read pairs where at least one mate is not ≥ 40 bp in length are discarded. Trimmed read pairs are mapped to the ETdb database used in a given experiment using bowtie2[20] with default parameters. Mappings are filtered to require a minimum identity ≥ 95% and minimum mapQ score ≥ 20, and coverage is calculated using a custom script, calc_cov.py, included with the ETsuite software.

647 Metagenomic sequencing for one biological replicate of the thiocyanate-degrading bioreactor
648 community (Conjugation - Control Sample - Replicate 3) failed. Metagenomic coverage values for
649 this replicate were generated by averaging the values from the other two biological replicates.
650

651 **ET-Seq normalization and calculation of insertion efficiency.**

652 To account for differences in sequencing depth, transposon junction PCR template amount, and
653 relative abundance of microbes in a community the data generated from both ET-Seq and
654 shotgun metagenomics were each normalized independently to values from the spike in control
655 organism, *B. thetaiotaomicron,* and then ET-Seq data is subsequently normalized by
656 metagenomic abundance as follows: Initially read count tables from ET-Seq and metagenomics
657 are filtered to remove any ET-Seq read count associated with < 2 barcodes and any metagenomic
658 read count < 10 reads. Next a size factor for each sample is calculated based on the geometric
659 mean of *B. thetaiotaomicron* reads for ET-Seq samples and *B. thetaiotaomicron* coverage for
660 metagenomics samples. ET-Seq read counts and metagenomic coverage values are then divided
661 by their respective sample size factors to create normalized values. Normalized ET-Seq read
662 counts are then divided by their paired normalized metagenomic coverage values to generate ET-
663 Seq read counts that are fully normalized to both ET-Seq sequencing depth and metagenomic
664 coverage. Finally fully normalized ET-Seq read counts for target organisms are divided by the
665 fully normalized ET-Seq read count of *B. thetaiotaomicron* from an experiment (a constant that
666 represents the number of reads that would be obtained from an organism with 100% of its
667 chromosomes carrying insertions). The resulting values for each target organism in a sample
668 represent an estimate of the fraction of that organism's population that received insertions
669 (Insertion Efficiency). Additionally, we multiply a target organism's insertion efficiency by the
670 fractional relative abundance of that organism in a sample, based on metagenomic data, to
671 estimate the fraction of an entire sample population that is made up of cells of a given species
672 that received insertions (Insertion-Receiving Fraction in Total Community).

673

674 **ET-Seq validation and establishing limits of detection and quantification**.

675 To validate ET-Seq and establish both a limit of detection (LOD) and limit of quantification (LOQ)
676 for the assay, a library of *K. michiganensis* transposon mutants was constructed by antibiotic
677 selection following conjugation with pHLL250 (as described above), and this library was added to
678 untransformed samples of the combined nine-member community to create a transformed cell
679 concentration gradient. Technical triplicate samples were created where 1%, 0.1%, 0.01%,
680 0.001% and 0% of the total *K. michiganensis* cells (by OD_{600}) in the mixture were those derived
681 from the transformed library. All samples (n = 15) were subjected to ET-Seq (as described above),
682 and pooled samples across all concentrations for each technical triplicate (n = 3; 5 concentrations)
683 were analyzed for community composition using shotgun metagenomics (as described above).
684 ET-Seq insertion efficiencies and insertion-receiving fraction in total community values were
685 averaged across technical replicates. Additionally, to derive the fraction of transformed *K.*
686 *michiganensis* cells that made up the total community (not just the *K. michiganensis* sub-
687 population), the known fraction of *K. michiganensis* cells that were transformed in a sample was
688 multiplied by the measured relative abundance of *K. michiganensis* in a given technical replicate,
689 and these values were averaged across technical replicates.

690 To derive the LOD and LOQ for ET-Seq a linear regression was performed using the lm
691 function in the base package of R[23] using the known fraction of transformed *K. michiganensis*
692 cells that made up the total community as the independent variable and the ET-Seq estimated
693 per community insertion efficiency as the dependent variable. The sample where transformed *K.*
694 *michiganensis* made up 0% of the community was not included in the regression analysis, but
695 was reserved to demonstrate zero response with no transformed cells present. LOD was
696 calculated as 3.3 * standard error of the regression / slope. The LOQ was calculated as 10 *
697 standard error of the regression / slope.

698

699 **Identification of positive transformations and statistical analysis**

700 For all ET-Seq experiments conducted we initially determined if any ET-Seq estimated per
701 community insertion efficiency was larger than the LOD. Values larger than the LOD constituted
702 a positive detection. For comparative statistical analysis conducted to compare insertion
703 efficiencies between transformation methods (Fig. 2b) only values that had a corresponding
704 insertion-receiving fraction in total community > LOQ were used. Statistical testing was conducted
705 using Analysis of Variance (ANOVA) implemented in the aov function in R[23]. Post-hoc testing was
706 conducted using the TukeyHSD function in R. Traditional 95% confidence intervals were
707 calculated using the groupwiseMean function of the rcompanion package in R.

708

709 **Multiple delivery experiments in communities**.

710 To test multiple delivery methods on the nine-member community, all members were grown at
711 30°C with *Bacillus sp. AnTP16* and *Methylobacterium sp. UNC378MF* in R2A liquid media while
712 all other members were inoculated in LB. Equal amounts of community members were then
713 combined by OD_{600}. This consortium then underwent transformation (of pHLL250), conjugation
714 (pHLL250 in WM3064), and electroporation of the pHLL250 vector (described in Delivery Methods
715 section). After delivery the community was spun down at 5,000*g* for 10 minutes, washed once
716 with LB and then spun down and frozen at -80°C until genomic DNA extraction.

717 The thiocyanate-degrading microbial community was sampled for delivery testing from biofilm on
718 a four liter continuously stirred tank reactor that had been maintained at steady state for over a
719 year. The reactor is operated with a two day hydraulic residence time, sparged with laboratory air
720 at 0.9 L/min, and fed with a mixture of molasses (0.15% w/v), thiocyanate (250 ppm), and KOH
721 to maintain pH 7. OD measurements were not feasible on the biofilm so we used its wet mass to
722 approximate equivalent OD and thus cell numbers to those used for the nine-member community.
723 This community underwent the same transformation, electroporation, and conjugation delivery
724 approaches as the nine-member community, however in all steps requiring media, LB was

725 replaced with molasses media (no thiocyanate). After delivery the community was spun down at
726 5,000*g* for 10 minutes, washed once with molasses media and then spun down and frozen at -
727 80°C until genomic DNA extraction.
728
729 **Benchmarking DART systems in *E. coli*.**
730 We first constructed several DART systems to identify variants capable of efficient transposition
731 by conjugative delivery to *E. coli*. We performed parallel conjugation of each DART vector variant
732 containing Gm^R Tn cargo (2.1 kbp) and either a non-targeting gRNA or one of two *lacZ*-targeting
733 gRNAs for each system. For VcDART, variation of the promoter controlling the expression of
734 VcCasTn components did not significantly impact transposition efficiency (Extended Data Fig. 4c-
735 d). Similarly for ShDART, expression of the sgRNA in three distinct transcriptional configurations
736 did not significantly impact transposition efficiency (Extended Data Fig. 4e-f). Since promoter and
737 transcriptional configuration variation had insignificant effects on transposition efficiency--and to
738 remove the requirement for promoter induction and reliance on T7 RNA polymerase--we
739 performed target specificity benchmarking of VcDART and ShDART using the same constitutive
740 P_{lac} promoter. In this experiment, ShDART Cas and Tns genes and sgRNA were encoded in the
741 original transcriptional configuration and under control of the same promoter in which ShCasTn
742 was first characterized by Strecker et al.[3].
743 The *lacZ*-targeting gRNAs were designed to target the *lacZ* α-peptide present in the
744 conjugation recipient strain *E. coli* BL21(DE3) but absent in the *lacZ*ΔM15 strains used as cloning
745 host (*E. coli* EC100D-*pir*+) or conjugation donor (*E. coli* WM3064), preventing transposition until
746 delivery into the recipient cell (Extended Data Fig. 4a). Donor WM3064 strains were transformed
747 and cultivated as described above, and recipient BL21(DE3) was inoculated from glycerol stock
748 into 100 mL LB in a 250 mL baffled shake flask at 37°C 250 rpm. Conjugations were performed
749 as described above using LB medium and 37°C incubation for every step, except that 0.1 mM
750 IPTG was added to VcDART conjugation plates in Extended Data Fig. 4d to induce transcription

751 from $P_{T7\text{-}lac}$ and T7 RNA polymerase expression in *E. coli* BL21(DE3). Transposition efficiencies
752 were calculated as the percentage of colonies resistant to 10 µg mL^{-1} gentamycin relative to viable
753 colonies in absence of gentamycin.

754 On/off-target analysis was performed for one *lacZ*-targeting guide for each DART system
755 by outgrowth under selection followed by genomic DNA extraction and ET-Seq. Specifically,
756 approximately 10,000 transconjugant cfu were plated on LB agar with gentamycin, incubated at
757 37°C overnight, scraped from agar into liquid LB medium, diluted to OD_{600} = 0.25 into 10 mL LB
758 plus gentamycin in 50 mL conical tubes, incubated at 37°C 250 rpm until OD_{600} = 1.0, centrifuged
759 at 4,000*g*, and frozen for downstream analysis. To determine the percent of selectable transposed
760 colonies possessing on-target and off-target edits, the total number of selectable colonies was
761 adjusted (Extended Data Fig. 4b) for on-target and off-target percent as determined by ET-Seq
762 (Fig. 4b). ET-Seq analysis was conducted on triplicate platings of DART transconjugants (n = 3
763 for each system) to identify transposon insertion locations and quantify on-target vs. off-target
764 insertions. As the targeted genomic region encoding the *lacZ* α-peptide is duplicated in *E. coli*
765 BL21(DE3), one of the two duplicated regions (749,903 bp --> 750,380 bp) was removed prior to
766 analysis to allow unambiguous mapping assignment. Subsequently, the standard ETsuite
767 analysis pipeline (as described above) was used to identify and map 300 bp X 2 reads containing
768 transposon junctions back to the recipient BL21(DE3) genome and cluster barcodes that
769 corresponded to unique insertion events. To confirm an insert location we first identified the exact
770 transposon-genome junction mapping coordinate that was the most frequent in the reads of a
771 barcode cluster (prime location) then required that a barcode cluster had: (1) at least 75% of its
772 reads coming from within 3 bp of the prime location and (2) at least 75% of its reads mapping to
773 the same strand. If these criteria were true the barcode cluster was counted as a unique insertion
774 and the prime location was used as the mapping locus by ET-Seq. An on-target insertion was
775 evaluated as a barcode cluster with a prime location within 200 bp downstream of the 3' end of

776 the protospacer target. Finally all distances reported from the protospacer target site were
777 calculated from the last base pair of the 3' end of the protospacer.
778
779 **VcDART-mediated targeted editing in a community**.
780 VcDART vectors encoding constitutive VcCasTn, constitutive *bla*:*aadA* Tn cargo (2.7 kbp), and
781 either a non-targeting (pBFC0888), *K. michiganensis* M5aI *pyrF*-targeting (pBFC0825), or *P.*
782 *simiae* WCS417 *pyrF*-targeting (pBFC0837) constitutive crRNA were transformed into *E. coli*
783 WM3064. Conjugations of these vectors into the nine-member community were performed as
784 described above on filter-topped LB agar plates with 12 hr incubation at 30°C. Lawns were
785 scraped from filters into 10 mL LB medium, vortexed, and 1 OD_{600}*mL from each lawn was plated
786 on LB agar supplemented with 1 mg mL^{-1} 5-FOA, 100 µg mL^{-1} carbenicillin, 100 µg mL^{-1}
787 streptomycin, and 100 µg mL^{-1} spectinomycin. Following 3 days of incubation at 30°C, all cells
788 were scraped from the agar into 10 mL R2A medium, vortexed, diluted into 10 mL R2A
789 supplemented with 20 mg mL^{-1} uracil (for no selection controls) or R2A with uracil, 5-FOA,
790 carbenicillin, streptomycin, and spectinomycin to OD_{600} = 0.02, and split evenly across 4 wells
791 (2.5 mL/well) of a 24 deep well plate. After cultivation at 30°C and 750 rpm for 1 week, only the
792 cultures conjugated with VcDART containing *pyrF*-targeting crRNA had grown in presence of
793 antibiotics and 5-FOA. A small portion of each of these cultures was serially diluted in R2A and
794 plated on LB agar plus antibiotics to isolate and assay colonies by targeted PCR and Sanger
795 sequencing of *pyrF* loci. The remainder of each culture was centrifuged at 4,000*g* for 10 min and
796 frozen at -80°C for downstream bacterial 16S rRNA V4 amplicon metagenomic sequencing
797 (Novogene). Relative abundances were calculated as described below (16S rRNA V4 amplicon
798 analysis) for pre-conjugation nine-member community cultures and post-selection *pyrF*-targeted
799 cultures.
800
801 **16S rRNA V4 amplicon analysis**

802 16S rRNA V4 amplicon sequencing was conducted using the 515F (5'-
803 GTGCCAGCMGCCGCGGTAA-3') and 806R (5'-GGACTACHVGGGTWTCTAAT-3') universal
804 bacterial primer set to generate 250 bp x 2 reads (Novogene). Samples were processed using
805 the UPARSE pipeline within the USEARCH software package to merge read pairs, remove
806 primers, quality filter sequences, remove chimeras, identify unique sequence variants (ZOTUs),
807 and quantify their abundance across samples as described previously[24]. To assign ZOTU
808 sequences to species known to be in our community mixture, we queried all 890 identified ZOTUs
809 against a custom database of 16S sequences derived from the genomes of the nine-member
810 community constituents using USEARCH[25] ZOTUs with 100% identity to a 16S sequence in our
811 database were assigned to the matched species, and all matches < 100% identity were counted
812 as "Other". Counts coming from ZOTUs of the same taxonomic assignment were merged and the
813 relative abundance of a species was calculated as its read counts divided by the total read counts
814 for the sample.
815
816 **Statistics and reproducibility**
817 All transformations (natural transformation, conjugation, electroporation) and subsequent
818 analyses were performed for three independent replicates.
819
820 **Reporting summary**
821 Further information on research design is available in the Nature Research Reporting Summary
822 linked to this paper.
823
824 **Data availability**
825 Summary data for genomes, plasmids, and oligonucleotides used in this study can be found in
826 Supplementary tables 1-4. Sequence data for all genomes assembled as part of this study and
827 newly constructed plasmids are in submission to NCBI with accession numbers pending.

828 Sequence data for genomes taken from Huddy, et al[8] are in submission to NCBI with accession
829 numbers pending. Sequence data for genomes taken from Kantor, et al[9] are available under NCBI
830 BioProject accession no. PRJNA279279. All genomes and plasmids used in the project will also
831 be made available on ggKbase (https://ggkbase.berkeley.edu/). Raw count data for all
832 experiments including both metagenome and ET-seq information is available at
833 https://github.com/SDmetagenomics/ETsuite/tree/master/manuscript_data.
834

835 **Code availability**

836 Custom R scripts for ET-Seq analysis and code used in the construction of figures are available
837 at https://github.com/SDmetagenomics/ETsuite.
838

839 **Methods references**

840 1. Adler, B. A. *et al.* Systematic Discovery of Salmonella Phage-Host Interactions via High-
841 Throughput Genome-Wide Screens. doi:10.1101/2020.04.27.058388.
842 2. Klompe, S. E., Vo, P. L. H., Halpin-Healy, T. S. & Sternberg, S. H. Transposon-encoded
843 CRISPR–Cas systems direct RNA-guided DNA integration. *Nature* **571**, 219–225 (2019).
844 3. Strecker, J. *et al.* RNA-guided DNA insertion with CRISPR-associated transposases.
845 *Science* **365**, 48–53 (2019).
846 4. Liu, H. *et al.* Magic Pools: Parallel Assessment of Transposon Delivery Vectors in Bacteria.
847 *mSystems* **3**, (2018).
848 5. Liu, H. *et al.* Large-scale chemical-genetics of the human gut bacterium Bacteroides
849 thetaiotaomicron. *BioRxiv* (2019).
850 6. Devon, R. S., Porteous, D. J. & Brookes, A. J. Splinkerettes--improved vectorettes for
851 greater efficiency in PCR walking. *Nucleic Acids Res.* **23**, 1644–1645 (1995).
852 7. Barquist, L. *et al.* The TraDIS toolkit: sequencing and analysis for dense transposon mutant

853 libraries. *Bioinformatics* **32**, 1109–1111 (2016).

854 8. Huddy, R. J. *et al.* Thiocyanate and organic carbon inputs drive convergent selection for
855 specific autotrophic Afipia and Thiobacillus strains within complex microbiomes. *bioRxiv*
856 2020.04.29.067207 (2020) doi:10.1101/2020.04.29.067207.

857 9. Kantor, R. S. *et al.* Genome-Resolved Meta-Omics Ties Microbial Dynamics to Process
858 Performance in Biotechnology for Thiocyanate Degradation. *Environ. Sci. Technol.* **51**,
859 2944–2953 (2017).

860 10. Olm, M. R., Brown, C. T., Brooks, B. & Banfield, J. F. dRep: a tool for fast and accurate
861 genomic comparisons that enables improved genome recovery from metagenomes through
862 de-replication. *ISME J.* **11**, 2864–2868 (2017).

863 11. Parks, D. H., Imelfort, M., Skennerton, C. T., Hugenholtz, P. & Tyson, G. W. CheckM:
864 assessing the quality of microbial genomes recovered from isolates, single cells, and
865 metagenomes. *Genome Res.* **25**, 1043–1055 (2015).

866 12. Chaumeil, P.-A., Mussig, A. J., Hugenholtz, P. & Parks, D. H. GTDB-Tk: a toolkit to classify
867 genomes with the Genome Taxonomy Database. *Bioinformatics* (2019)
868 doi:10.1093/bioinformatics/btz848.

869 13. Diamond, S. *et al.* Mediterranean grassland soil C-N compound turnover is dependent on
870 rainfall and depth, and is mediated by genomically divergent microorganisms. *Nat Microbiol*
871 **4**, 1356–1367 (2019).

872 14. Edgar, R. C. MUSCLE: multiple sequence alignment with high accuracy and high
873 throughput. *Nucleic Acids Res.* **32**, 1792–1797 (2004).

874 15. Nguyen, L.-T., Schmidt, H. A., von Haeseler, A. & Minh, B. Q. IQ-TREE: a fast and effective
875 stochastic algorithm for estimating maximum-likelihood phylogenies. *Mol. Biol. Evol.* **32**,
876 268–274 (2015).

877 16. Peng, Y., Leung, H. C. M., Yiu, S. M. & Chin, F. Y. L. IDBA-UD: a de novo assembler for
878 single-cell and metagenomic sequencing data with highly uneven depth. *Bioinformatics* **28**,

879 1420–1428 (2012).
880 17. Hyatt, D. *et al.* Prodigal: prokaryotic gene recognition and translation initiation site
881 identification. *BMC Bioinformatics* **11**, 119 (2010).
882 18. Lowe, T. M. & Eddy, S. R. tRNAscan-SE: a program for improved detection of transfer RNA
883 genes in genomic sequence. *Nucleic Acids Res.* **25**, 955–964 (1997).
884 19. Martin, M. Cutadapt removes adapter sequences from high-throughput sequencing reads.
885 *EMBnet.journal* **17**, 10–12 (2011).
886 20. Langmead, B. & Salzberg, S. L. Fast gapped-read alignment with Bowtie 2. *Nat. Methods*
887 **9**, 357–359 (2012).
888 21. Zhao, L., Liu, Z., Levy, S. F. & Wu, S. Bartender: a fast and accurate clustering algorithm to
889 count barcode reads. *Bioinformatics* **34**, 739–747 (2018).
890 22. Costello, M. *et al.* Characterization and remediation of sample index swaps by non-
891 redundant dual indexing on massively parallel sequencing platforms. *BMC Genomics* **19**,
892 332 (2018).
893 23. R Core Team. R: A language and environment for statistical computing. (2013).
894 24. Edgar, R. C. UPARSE: highly accurate OTU sequences from microbial amplicon reads.
895 *Nat. Methods* **10**, 996–998 (2013).
896 25. Edgar, R. C. Search and clustering orders of magnitude faster than BLAST. *Bioinformatics*
897 **26**, 2460–2461 (2010).

898

899 **Acknowledgments**

900 We thank Morgan N. Price for data analysis input, Patrick Pausch for experimental advice, Shana
901 L. McDevitt, Eileen Wagner, and Hitomi Asahara for help with sequencing, and Trent R. Northen
902 for directional advice. Funding was provided by m-CAFEs Microbial Community Analysis &
903 Functional Evaluation in Soils, (m-CAFEs@lbl.gov) a project led by Lawrence Berkeley National

904 Laboratory supported by the U.S. Department of Energy, Office of Science, Office of Biological &
905 Environmental Research under contract number DE-AC02-05CH11231. Support was also
906 provided by the Innovative Genomics Institute at UC Berkeley. B.E.R. and B.F.C. are supported
907 by the National Institute of General Medical Sciences of the National Institute of Health under
908 award numbers F32GM134694 and F32GM131654. Schematics were created with
909 BioRender.com.

910

911 **Contributions**

912 B.E.R., S.D., B.F.C, A.M.D., J.F.B, and J.A.D. conceived the work and designed the experiments.
913 B.E.R., B.F.C., C.H., M.X., Z.Z., D.C.S., K.T., T.K.O., and N.K. conducted the molecular biology
914 included. S.D., A.C.-C., C.H., and R.S. developed the bioinformatic analysis. B.E.R., S.D., B.F.C.,
915 A.M.D., J.F.B., and J.A.D. analyzed and interpreted the data.

916

917 **Competing Interests**

918 The Regents of the University of California have patents pending related to this work on which
919 B.E.R., S.D., B.F.C., A.M.D., J.F.B., and J.A.D. are inventors. J.A.D. is a co-founder of Caribou
920 Biosciences, Editas Medicine, Intellia Therapeutics, Scribe Therapeutics and Mammoth
921 Biosciences, a scientific advisory board member of Caribou Biosciences, Intellia Therapeutics,
922 eFFECTOR Therapeutics, Scribe Therapeutics, Synthego, Mammoth Biosciences and Inari, and
923 is a Director at Johnson & Johnson and has sponsored research projects by Biogen, Roche and
924 Pfizer. J.F.B. is a founder of Metagenomi.

925

926 **Additional Information**

927 Correspondence and request for materials should be addressed to J.A.D. and J.F.B.

928 # Extended Data

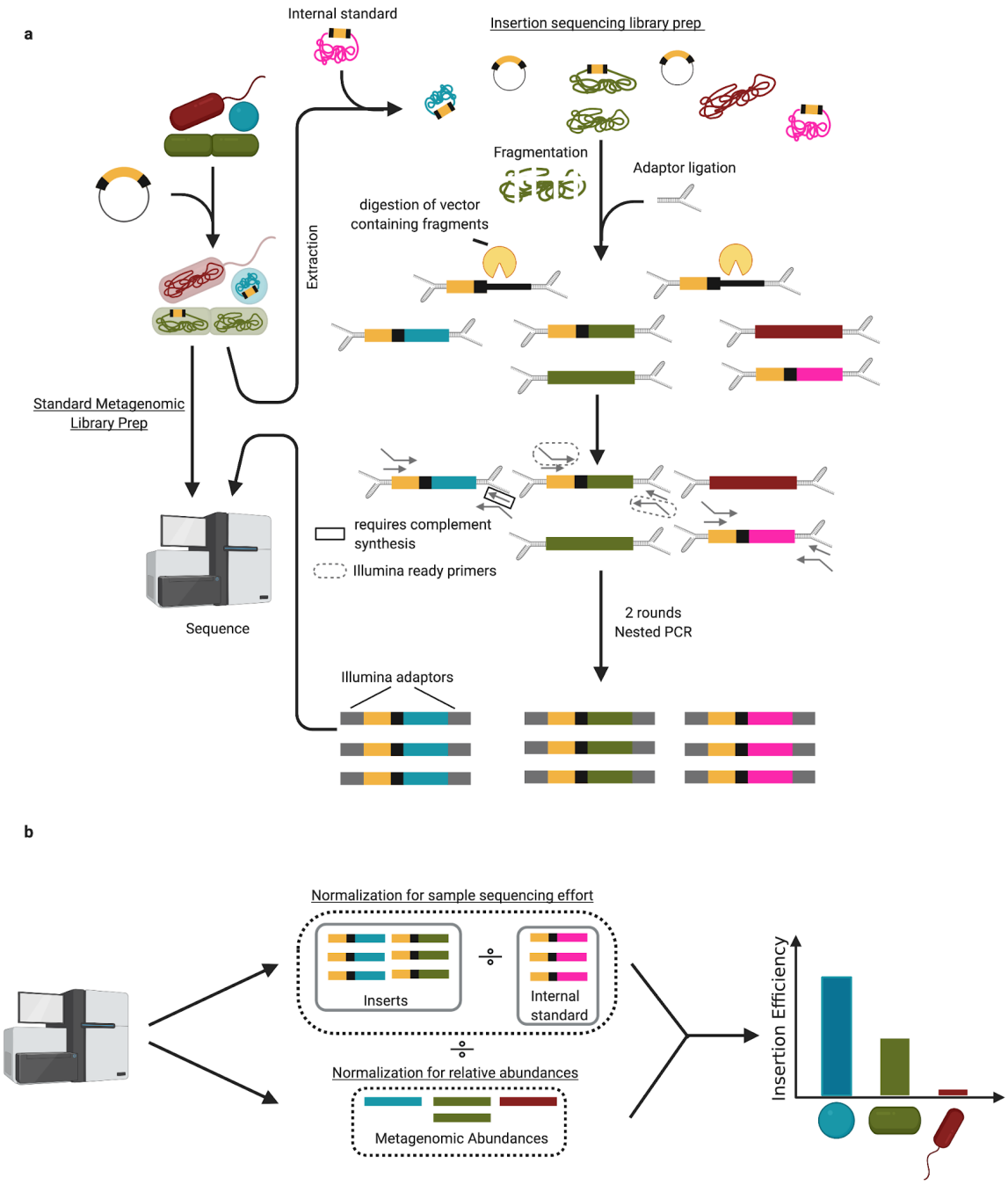

929

930 **Extended Data Fig. 1 | Library preparation and data normalization for ET-Seq. a**, ET-Seq requires low-
931 coverage metagenomic sequencing and customized insertion sequencing. Insertion sequencing relies on
932 custom splinkerette adaptors, which minimize non-specific amplification, a digestion step for degradation
933 of delivery vector containing fragments, and nested PCR to enrich for fragments containing insertions with

934 high specificity. The second round of nested PCR adds unique dual index adaptors for Illumina sequencing.
935 **b**, This insertion sequencing data is first normalized by the reads to internal standard DNA which is added
936 equally to all samples and serves to correct for variation in reads produced per sample. Secondly, it is
937 normalized by the relative metagenomic abundances of the community members.

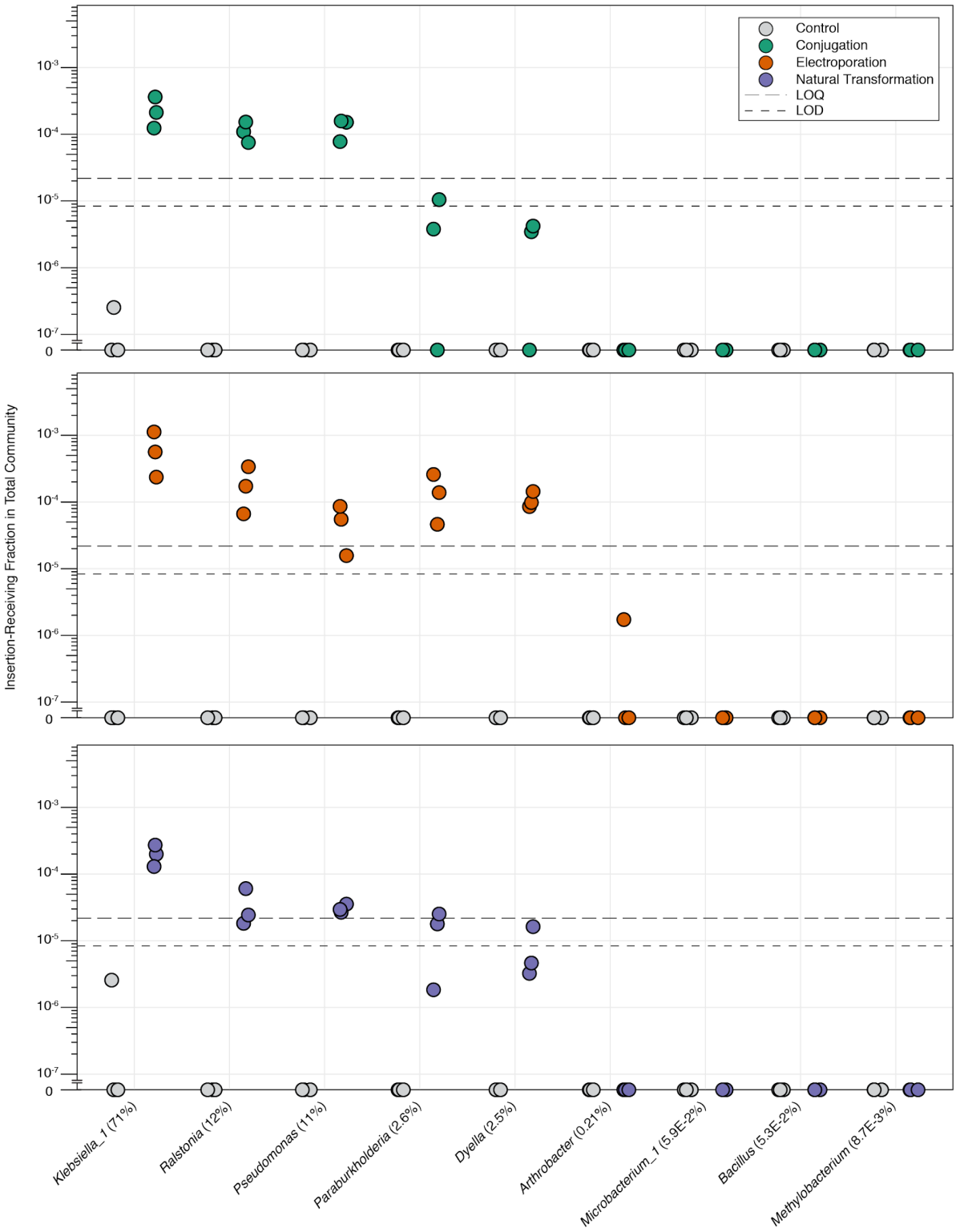

938

939 **Extended Data Fig. 2 | ET-Seq determined insertion efficiencies for all nine consortium members as**

940 **a fraction of the entire community.** ET-Seq determined insertion efficiencies for conjugation,

941 electroporation, and natural transformation on the nine-member synthetic community (n = 3 biological
942 replicates). The values shown are the estimated fraction a constituent species's transformed cells make of
943 the total community population. Control samples received no exogenous DNA. Average relative abundance
944 across all samples is indicated in parentheses (n = 18 independent samples). LOD and LOQ are indicated
945 in plots by short and long dashed lines respectively.
946

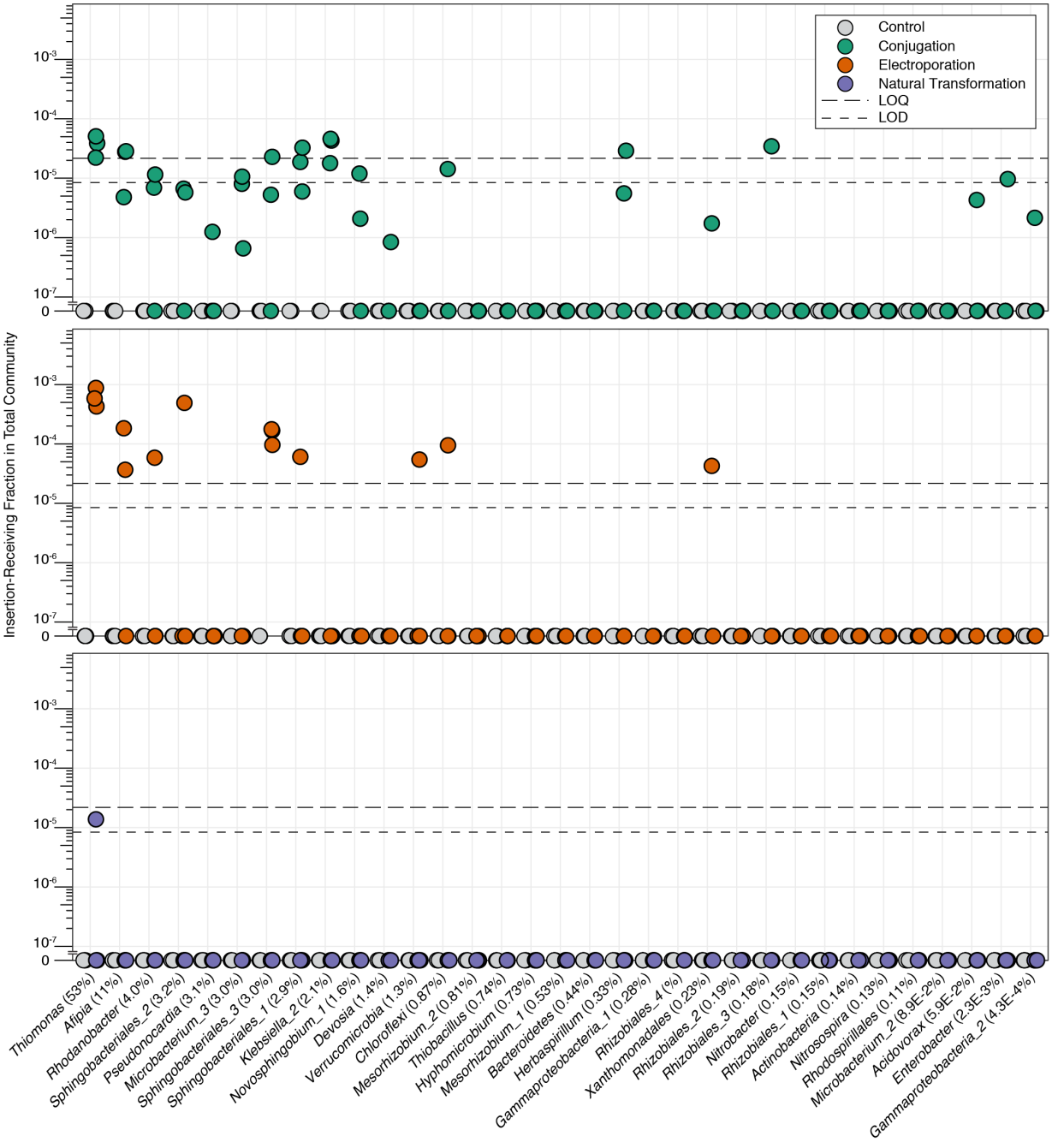

Extended Data Fig. 3 | ET-Seq determined insertion efficiencies for all thiocyanate-degrading bioreactor community members as a fraction of the entire community. ET-Seq determined insertion efficiencies for conjugation, electroporation, and natural transformation on the thiocyanate-degrading bioreactor community (n = 3 biological replicates). The values shown are the estimated fraction a constituent species's transformed cells make of the total community population. Control samples received

954 no exogenous DNA. Average relative abundance across all samples is indicated in parentheses (n = 17
955 independent samples; due to a single failed metagenomic sequencing replicate, see methods). LOD and
956 LOQ are indicated in plots by short and long dashed lines respectively.

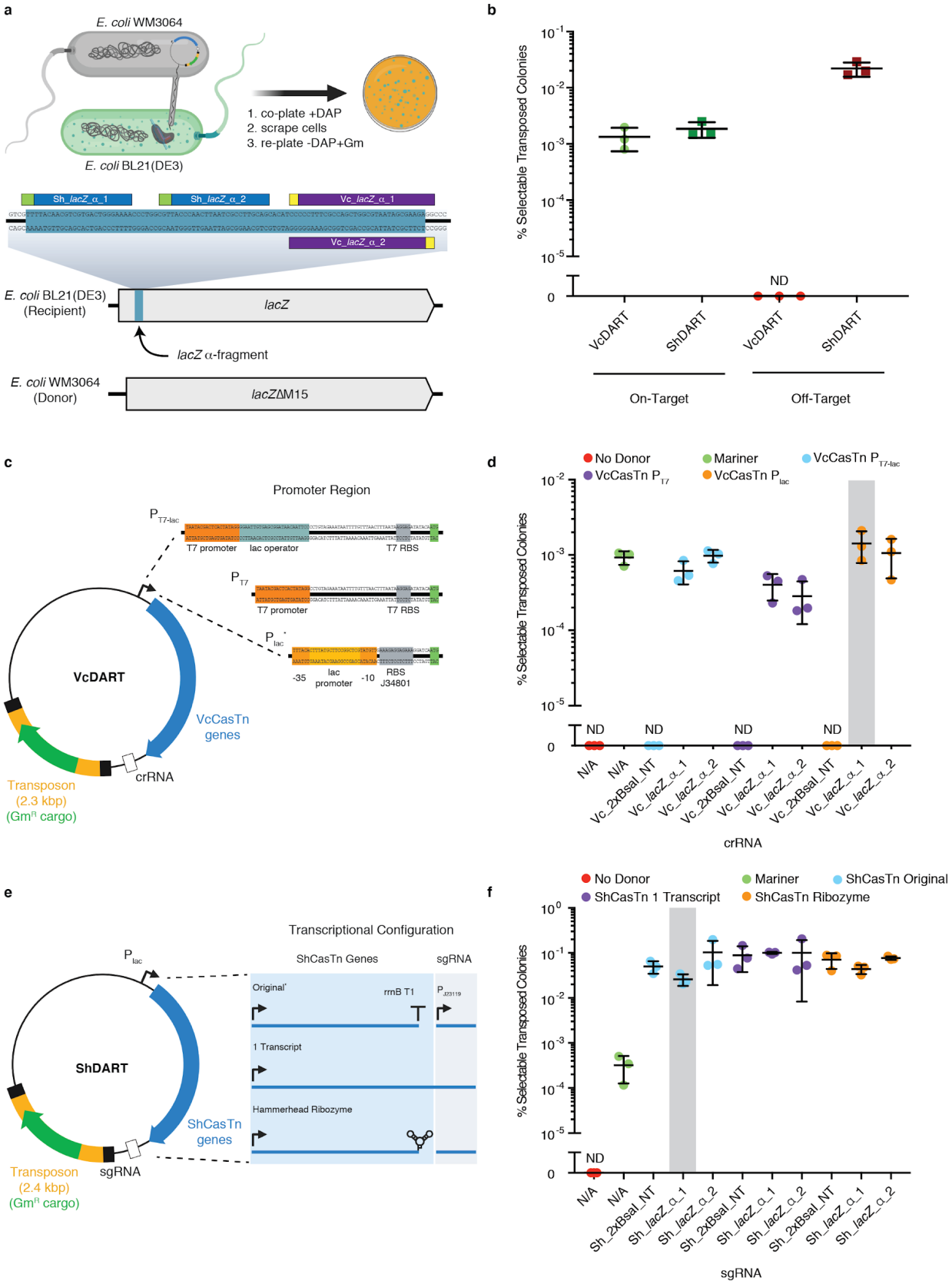
a
E. coli WM3064
1. co-plate +DAP
2. scrape cells
3. re-plate -DAP+Gm
E. coli BL21(DE3)
Sh_lacZ_α_1
Sh_lacZ_α_2
Vc_lacZ_α_1
Vc_lacZ_α_2
E. coli BL21(DE3) (Recipient)
lacZ
lacZ α-fragment
E. coli WM3064 (Donor)
lacZΔM15
b
% Selectable Transposed Colonies
ND
VcDART
ShDART
VcDART
ShDART
On-Target
Off-Target
c
Promoter Region
T7 promoter
lac operator
T7 RBS
T7 promoter
T7 RBS
-35
lac promoter
-10
RBS J34801
VcDART
VcCasTn genes
crRNA
Transposon (2.3 kbp) (GmR cargo)
d
No Donor
Mariner
VcCasTn P T7-lac
VcCasTn P T7
VcCasTn P lac
% Selectable Transposed Colonies
ND
N/A
N/A
Vc_2xBsaI_NT
Vc_lacZ_α_1
Vc_lacZ_α_2
crRNA
e
Transcriptional Configuration
ShCasTn Genes
sgRNA
Original
rrnB T1
1 Transcript
Hammerhead Ribozyme
ShDART
ShCasTn genes
sgRNA
Transposon (2.4 kbp) (GmR cargo)
f
No Donor
Mariner
ShCasTn Original
ShCasTn 1 Transcript
ShCasTn Ribozyme
% Selectable Transposed Colonies
ND
N/A
N/A
Sh_2xBsaI_NT
Sh_lacZ_α_1
Sh_lacZ_α_2
sgRNA

957

958 **Extended Data Fig. 4 | Benchmarking DART vectors. a,** *E. coli* WM3064 to *E. coli* BL21(DE3) conjugation,
959 transposition, and selection schematic (top) and guide RNAs targeting the *lacZ* α-fragment of recipient BL21(DE3),
960 which is absent from donor WM3064 (bottom). **b,d,f,** Percent selectable transposed colonies is calculated as the
961 number of colonies obtained with gentamycin selection divided by total viable colonies in absence of selection. **b,**
962 Insertion receiving colonies divided into on- and off-targeted. This was calculated by multiplying % selectable colonies
963 for representative guides in **d** and **f** (highlighted by grey bars) by the on- or off-target rates (shown in Fig. 4). **c**,
964 Transposition with VcDART was tested with three promoters. The variant using the P_{lac} promoter, harvested from
965 pHelper_ShCAST_sgRNA[18], was also used for Fig. 4, 5, and Extended Data Fig. 4b (*). **d,** Efficiencies of VcDART
966 using various promoters. **e,** Transposition with ShDART was tested with three transcriptional configurations, all using
967 P_{lac}[18]. The configuration used for characterization of ShCasTn originally[18] was also used for Fig. 4 and Extended Data
968 Fig. 4b (*). **f,** Efficiencies of ShDART using various promoters. **b, d, f,** Crossbar indicates mean and error bars indicate
969 one standard deviation from the mean (n = 3 biological replicates). Guide RNAs ending in "NT" are non-targeting
970 negative control samples.